Cancer Cell

Article

Durvalumab with olaparib and paclitaxel for high-risk HER2-negative stage II/III breast cancer: Results from the adaptively randomized I-SPY2 trial

Graphical abstract

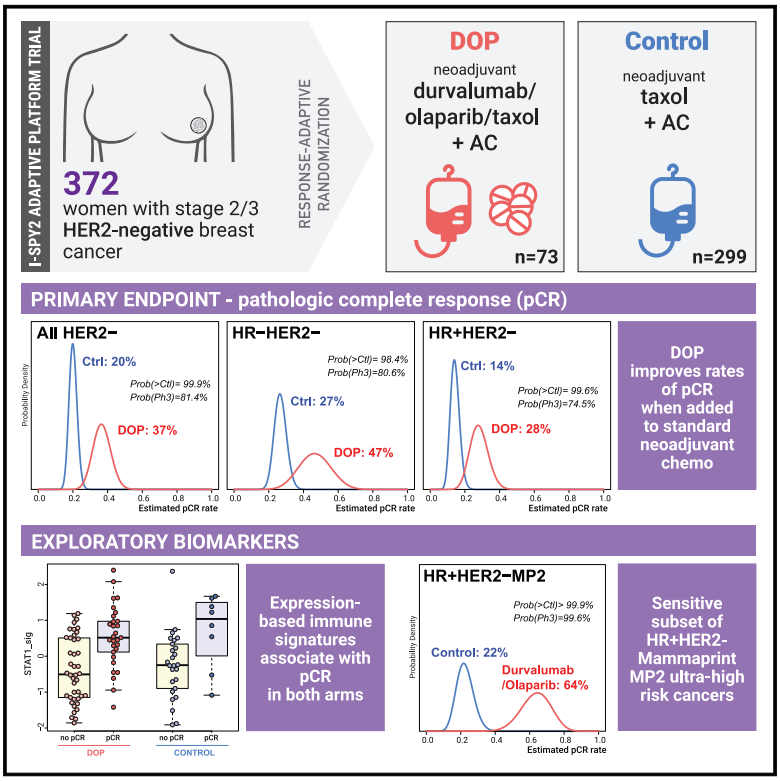

Highlights

- Durvalumab plus olaparib improved chemotherapy efficacy in HER2-negative breast cancer
- Immune-rich tumors had greater sensitivity to therapy
- Among ER+ cancer, only Mammaprint MP2 cancers benefited from immune checkpoint therapy

Authors

Lajos Pusztai, Christina Yau, Denise M. Wolf, ..., Angela M. DeMichele, Donald A. Berry, Laura J. Esserman

Correspondence

lajos.pusztai@yale.edu

In brief

Pusztai et al. report findings from the I-SPY2 trial showing durvalumab and olaparib administered with paclitaxel improved pathologic complete response (pCR) rate in HER2-negative breast cancers, including TNBC and ER-positive cancers. Among the ER-positive/HER2-negative cancers, only the highly proliferative, estrogen receptor low, MammaPrint MP2 subset benefited from the combination therapy.

Pusztai et al., 2021, Cancer Cell *39*, 989–998
July 12, 2021
https://doi.org/10.1016/j.ccell.2021.05.009

CellPress

Cancer Cell

CellPress

Article

Durvalumab with olaparib and paclitaxel for high-risk HER2-negative stage II/III breast cancer: Results from the adaptively randomized I-SPY2 trial

Lajos Pusztai,[1,23,*] Christina Yau,[2] Denise M. Wolf,[3] Hyo S. Han,[4] Lili Du,[5] Anne M. Wallace,[6] Erica String-Reasor,[7] Judy C. Boughey,[8] A. Jo Chien,[2] Anthony D. Elias,[9] Heather Beckwith,[10] Rita Nanda,[11] Kathy S. Albain,[12] Amy S. Clark,[13] Kathleen Kemmer,[14] Kevin Kalinsky,[15] Claudine Isaacs,[16] Alexandra Thomas,[17] Rebecca Shatsky,[6] Theresa L. Helsten,[18] Andres Forero-Torres,[7] Minetta C. Liu,[8] Lamorna Brown-Swigart,[3] Emmanuel F. Petricoin,[19] Julia D. Wulfkuhle,[19] Smita M. Asare,[20] Amy Wilson,[20] Ruby Singhrao,[2] Laura Sit,[2] Gillian L. Hirst,[2] Scott Berry,[21] Ashish Sanil,[21] Adam L. Asare,[20] Jeffrey B. Matthews,[2] Jane Perlmutter,[22] Michelle Melisko,[2] Hope S. Rugo,[2] Richard B. Schwab,[18] W. Fraser Symmans,[5] Doug Yee,[10] Laura J. van't Veer,[2] Nola M. Hylton,[2] Angela M. DeMichele,[13] Donald A. Berry,[21] and Laura J. Esserman[2]

[1]Breast Medical Oncology, Yale Cancer Center, Yale School of Medicine, 333 Cedar Steet, PO Box 208032, New Haven, CT 06510, USA
[2]Helen Diller Family Comprehensive Cancer Center, University of California, San Francisco, CA 94143, USA
[3]Department of Laboratory Medicine, University of California, San Francisco, CA 94143, USA
[4]Medical Oncology, Moffitt Cancer Center, Tampa, FL 33612, USA
[5]Department of Pathology, University of Texas MD Anderson Cancer Center, Houston, TX 77030, USA
[6]Comprehensive Breast Health Center, University of California San Diego, La Jolla, CA 92037, USA
[7]Department of Hematology & Oncology, University of Alabama at Birmingham, Birmingham, AL 35233, USA
[8]Department of Surgery, Mayo Clinic, Rochester, MN 55905, USA
[9]Department of Internal Medicine, University of Colorado, Aurora, CO 80045, USA
[10]Masonic Cancer Center, University of Minnesota, Minneapolis, MN 55455, USA
[11]Department of Medicine, University of Chicago, Chicago, IL 60637, USA
[12]Hematology/Oncology, Loyola University Chicago Stritch School of Medicine, Chicago, IL 60153, USA
[13]Abramson Cancer Center, University of Pennsylvania, Philadelphia, PA 19104, USA
[14]Knight Cancer Institute, Oregon Health & Sciences University, Portland, OR 97239, USA
[15]Herbert Irving Comprehensive Cancer Center, Columbia University, New York, NY 10032, USA
[16]Lombardi Comprehensive Care Center, Georgetown University, Washington, DC 20007, USA
[17]Medical Oncology and Hematology, Wake Forest University, Winston-Salem, NC 27157, USA
[18]Moores Cancer Center, University of California San Diego, La Jolla, CA 92037, USA
[19]Center for Applied Proteomics and Molecular Medicine, George Mason University, Manassas, VA 20110, USA
[20]Quantum Leap Healthcare Collaborative, San Francisco, CA 94118, USA
[21]Berry Consultants, LLC, Austin, TX 78746, USA
[22]Gemini Group, Ann Arbor, MI 48107, USA
[23]Lead contact
*Correspondence: lajos.pusztai@yale.edu
https://doi.org/10.1016/j.ccell.2021.05.009

SUMMARY

The combination of PD-L1 inhibitor durvalumab and PARP inhibitor olaparib added to standard paclitaxel neoadjuvant chemotherapy (durvalumab/olaparib/paclitaxel [DOP]) was investigated in the phase II I-SPY2 trial of stage II/III HER2-negative breast cancer. Seventy-three participants were randomized to DOP and 299 to standard of care (paclitaxel) control. DOP increased pathologic complete response (pCR) rates in all HER2-negative (20%–37%), hormone receptor (HR)-positive/HER2-negative (14%–28%), and triple-negative breast cancer (TNBC) (27%–47%). In HR-positive/HER2-negative cancers, MammaPrint ultra-high (MP2) cases benefited selectively from DOP (pCR 64% versus 22%), no benefit was seen in MP1 cancers (pCR 9% versus 10%). Overall, 12.3% of patients in the DOP arm experienced immune-related grade 3 adverse events versus 1.3% in control. Gene expression signatures associated with immune response were positively associated with pCR in both arms, while a mast cell signature was associated with non-pCR. DOP has superior efficacy over standard neoadjuvant chemotherapy in HER2-negative breast cancer, particularly in a highly sensitive subset of high-risk HR-positive/HER2-negative patients.

INTRODUCTION

Several studies indicate that the addition of immune checkpoint inhibitors to standard of care chemotherapy can improve pathologic complete response (pCR) rates in stage II–III triple-negative breast cancer (TNBC). In a previous arm of the I-SPY2 trial, four cycles of pembrolizumab added to standard paclitaxel-based neoadjuvant chemotherapy improved estimated

Table 1. Demographics and baseline characteristics of participants

Characteristic	Duvalumab/olaparib (n = 73)	Control (n = 299)
Median age, year (range)	46 (28–71)	48 (24–80)
Ethnicity		
White	59 (81%)	234 (78%)
African American	8 (11%)	40 (13%)
Asian	6 (8%)	22 (7%)
Other/mixed	0 (0%)	3 (1%)
HR status		
Positive	52 (71%)	157 (53%)
Negative	21 (29%)	142 (47%)
MammaPrint		
MP1	26 (36%)	133 (44%)
MP2	47 (64%)	166 (56%)
Median tumor size, cm (range)	3.7 (1.9–13)	3.8 (1.2–15)
Baseline node status		
Palpable	21 (29%)	109 (36%)
Non-palpable	19 (26%)	129 (43%)
N/A	33 (45%)	61 (20%)

HR, hormone receptor; N/A, not applicable.

pCR rate from 22% to 60% in TNBC (Nanda et al., 2020). A subsequent randomized phase III trial confirmed a significantly higher pCR rate (64.8% versus 51.2%) when pembrolizumab was added to chemotherapy; preliminary results suggest improved recurrence-free survival (hazard ratio = 0.63) in TNBC (Schmid et al., 2020). Durvalumab, an anti-programmed death-ligand 1 (PD-L1) monoclonal antibody, has received FDA approval for bladder and lung cancers (Stewart et al., 2015). In a single-arm, single-institution, phase I/II neoadjuvant trial (n = 59) of stage I–III TNBC, when durvalumab was administered concurrent with weekly nab-paclitaxel and followed by dose-dense doxorubicin/cyclophosphamide (AC), the final pCR rate was 44%, with no dose-limiting toxicities observed (Foldi et al., 2021). A randomized phase II study in TNBC (n = 174), GeparNuevo, demonstrated a numerical, but not statistically significant, increase in pCR rate (53.4% versus 44.2%, p = 0.287) when durvalumab was added to weekly nab-paclitaxel followed by epirubicin/cyclophosphamide neoadjuvant chemotherapy (Loibl et al., 2019). The safety and efficacy of the combination of durvalumab and olaparib (a polyadenosine 5′-diphosphoribose polymerase [PARP] inhibitor) were established in the MEDIOLA (NCT02734004) phase I/II multi-cohort basket trial. Preliminary results of the germline *BRCA* mutant metastatic breast cancer cohort of the trial indicated good tolerability and an objective tumor response rate of 59% (Domchek et al., 2020).

Preclinical studies suggest the potential for synergistic improvement using a combination of immune checkpoint inhibitors and PARP inhibitors (Esteva et al., 2019). Impaired nucleotide and base excision repair caused by PARP inhibition can increase mutation and neoantigen loads that are associated with increased sensitivity to immune checkpoint therapy (Lassen, 2019). DNA fragments generated by impaired DNA repair can also activate the intracellular stimulator of interferon genes pathway in cancer cells, leading to signaling events that activate immune cells in the tumor microenvironment (Pantelidou et al., 2019).

Here, we report the results of an arm of the neoadjuvant I-SPY2 adaptive platform trial for stage II/III early breast cancer evaluating a combination of durvalumab and olaparib. Our goal was to estimate if the combination of durvalumab and olaparib concurrent with weekly paclitaxel neoadjuvant therapy (durvalumab/olaparib/paclitaxel [DOP]) could increase the pCR rate compared with chemotherapy alone in HER2-negative, stage II–III breast cancers. *A priori* defined and exploratory molecular markers were also assessed to identify predictive markers. The primary endpoint was pathologic complete response (pCR), and *a priori* defined and exploratory molecular markers were assessed for the purpose of identifying biomarkers predictive of response. I-SPY is a multi-arm, adaptively randomized trial that aims to rapidly identify new drug combinations that induce higher pCR rates than standard of care chemotherapy in various breast cancer biomarker subsets (Barker et al., 2009). The pCR rates are monitored in real time, along with early imaging response, as they accumulate in each arm and Bayesian adoptive randomization ensures that patients are preferentially accrued to arms with higher pCR rates. A minimum proportion (20%) of patients are continuously allocated to the control arm (chemotherapy alone). This design allows rapid identification of promising new therapies in *a priori* defined biomarker subtypes with a smaller sample size than traditional randomized phase II trials. An arm is considered successful and "graduate" when, based on the accumulating responses, the statistical engine predicts an $\geq$85% probability that the experimental arm would have a statistically significantly higher pCR rate than the control arm in a 300-patient traditional 1:1 randomized trial. An arm could graduate in one or more biomarkers subsets.

RESULTS

Efficacy

Between May 3, 2018, and June 2, 2019, 73 HER2-negative patients (21 TNBC, 52 HR-positive/HER2-negative) were enrolled in the DOP arm. Three hundred and thirty-six participants were randomized to the control arm (paclitaxel) but 37 did not receive the allocated treatment, resulting in 299 evaluable HER2-negative patients in the control arm (CONSORT diagram, Figure S1). Baseline characteristics were similar between the experimental and control arms (Table 1). Seventeen patients in the control arm and one in the experimental arm did not proceed to surgery (due to patient's choice, leaving the treating institution, or progression) and were considered non-pCR for primary efficacy analysis.

On June 2, 2019, the prespecified Bayesian modeling of surgical pathology results and serial MRI assessments from the first 23 of the 73 patients predicted that the probability of success in a hypothetical phase III trial were 0.944, 0.950, and 0.838 in all HER2-negative, HR-positive/HER2-negative, and TNBC subtypes, respectively. Per protocol, further accrual was therefore stopped and DOP graduated in the HER2-negative, and HR-positive/HER2-negative signatures. After all patients

subsequently completed surgery, the final efficacy analysis indicated that durvalumab plus olaparib improved estimated pCR rates (over control) from 20% to 37% in HER2-negative cancers, from 14% to 28% in HR-positive/HER2-negative cancers, and from 27% to 47% in TNBC. Final probability distributions for achieving pCR are shown in Figure 1A, including the 95% probability intervals. Final predicted probabilities of phase III success were 0.814, 0.745, and 0.806 in all HER2-negative, HR-positive/HER2-negative, and TNBC signatures, respectively, after all participants had completed surgery. The overall probability that the experimental arm was superior to the control was >98% for all three signatures.

DOP also shifted residual cancer burden (RCB) categories toward lower values across the entire range of RCB scores (Symmans et al., 2017). The proportion of patients in RCB II and III categories (i.e., moderate and extensive residual disease) were lower in the DOP arm, indicating smaller residual cancers across the entire residual disease spectrum in all subsets (Figure 1B).

Median follow-up duration for participants in the experimental arm at the time of submission was 18 months, thus distant metastasis-free and overall survival results are not yet mature.

Safety and toxicity

All patients who received at least one dose of study-assigned therapy were evaluable for safety and toxicity. In the control arm, 34% (n = 102) and in the experimental arm 56% (n = 41) of patients experienced at least one grade $\geq$3 adverse event. Grade 3 and 4 adverse events are summarized in Table 2 (also see Data S1, "Frequency of all adverse events observed"). Immune-related adverse events were more common in the experimental arm; 9 patients (12%) in the DOP arm experienced immune-related grade 3 or greater adverse events compared with 4 patients (1.3%) in the control arm. Overall, 20 patients (27.4%) experienced an immune-related adverse event (grades 1 through 4) in the experimental arm compared with 6 patients (2%) in the control arm. In the experimental arm, immune-related adverse events included 5 patients (7%) with hypothyroidism (grade 1 and 2), 4 (5%) pneumonitis (grade 1/2), 4 (5%) adrenal insufficiency (1 patient with grade 1 and 3 with grade 3), and 1 each of non-insulin-dependent diabetes (grade 1), thyroiditis (grade 3), and pancreatitis (grade 3). Dose reductions and early discontinuation of therapy are also shown in Table 2. The median time from treatment consent to surgery was similar in the experimental (168 days, range: 107–273) and control arms (165 days, range: 85–289).

Biomarker analysis

Seventy-one participants in the DOP arm and 34 assigned to control had expression data from pre-treatment formalin-fixed paraffin-embedded biopsies available for biomarker analysis. Thirteen *a priori* defined mRNA biomarkers (Table S1), including 10 immune signatures, and one proliferation, DNA repair, and estrogen receptor (ER) signature each, were examined as predictive markers. In the whole biomarker population, 7 and 5 of the 10 immune mRNA markers studied were significantly associated with higher pCR rate in the experimental and control arms, respectively (Figure 2). The DNA repair deficiency (PARPi7) and mitotic signatures (described in Table S1) were also positively associated with pCR but only in the experimental arm. The T cell signature and CD68 mRNA expression showed no significant association with pCR in either treatment arm, and the dendritic cell signature was only significant in the experimental arm. The mast cell signature and ESR1/PGR expression were significantly associated with lack of pCR in the experimental arm and showed a similar but non-significant trend for the same direction in the control arm. The marker-treatment interaction tests were not significant for nearly all of these markers (9/10), indicating that they cannot identify the patient population that selectively benefited from inclusion of durvalumab and olaparib. We also note that the expression of 8 of the 10 immune markers were highly positively correlated with one another, only the mast cell and macrophage/T cell ratio signatures showed weak or negative correlation with the other immune markers. ESR1 expression also correlated negatively with all other markers except the mast cell signature (Figure S2). Pairwise comparisons of the 13 mRNA biomarkers between cases of pCR and no-PCR by treatment arm in the whole study population, and in the TNBC and HR-positive/HER2-negative subsets, respectively, are shown in Figures S3–S5. Associations between the 13 mRNA biomarkers and pathologic response in the whole biomarker study population, and in the TNBC and HR-positive/HER-negative subsets are shown in Table S2.

In the TNBC subset (N = 21 DOP, N = 19 control), the STAT1, macrophage/T cell, and mitotic signatures were positively associated with pCR in the experimental arm, and no marker was associated with response in the control arm (Figure 2). However, the marker-treatment interaction tests were not significant. The only immune marker that was associated with lack of pCR in both treatment arms was high expression of the mast cell signature.

In the HR-positive/HER2-negative subset (N = 50 durvalumab/olaparib, N = 15 control), high ESR1, PGR expression, and mast cell signature were associated with lack of pCR, and all other markers except CD68 (which was not associated with response) were positively associated with pCR in the experimental arm (Figure 2). There were too few pCRs (N = 2) in the control arm in this biomarker cohort to perform analysis. We also examined predicted pCR rates in the two MammaPrint subsets, MP1 (N = 109 control, N = 24 experimental arm) and MP2 (N = 49 control, N = 28 experimental). The MP2 subgroup, corresponding to 53% of the MammaPrint high, HR-positive/HER2-negative subset in this trial arm, derived all the benefit from adding durvalumab and olaparib to chemotherapy, in this subset the predicted pCR probabilities were 64% (95% CI: 47%–80%) and 22% (95% CI: 13%–32%) in the experimental and control arms, respectively (Figures 3A and 3B). Patients in the MP1 group had low pCR rates in both arms and showed no improvement with DOP (9% versus 10%); the RCB score distributions in the MP1 and MP2 subsets are shown in Figure S4. Because, in HR-positive cancers, ER signaling and proliferation determine endocrine and chemotherapy sensitivities, respectively, we compared expression levels of the proliferation and $SET_{ER/PR}$ gene signatures between the MP1 and MP2 HR-positive/HER2-negative cancers. We also assessed if the MP1 and MP2 subtypes differ in immune gene expression using the tumor inflammation signature as a general marker of immune presence. We selected this signature because it showed the highest correlation with other immune signatures and has also been extensively validated as marker of immunotherapy response in clinical trial tissues (Ayers et al., 2017). The MP2 subset had significantly higher proliferation and significantly

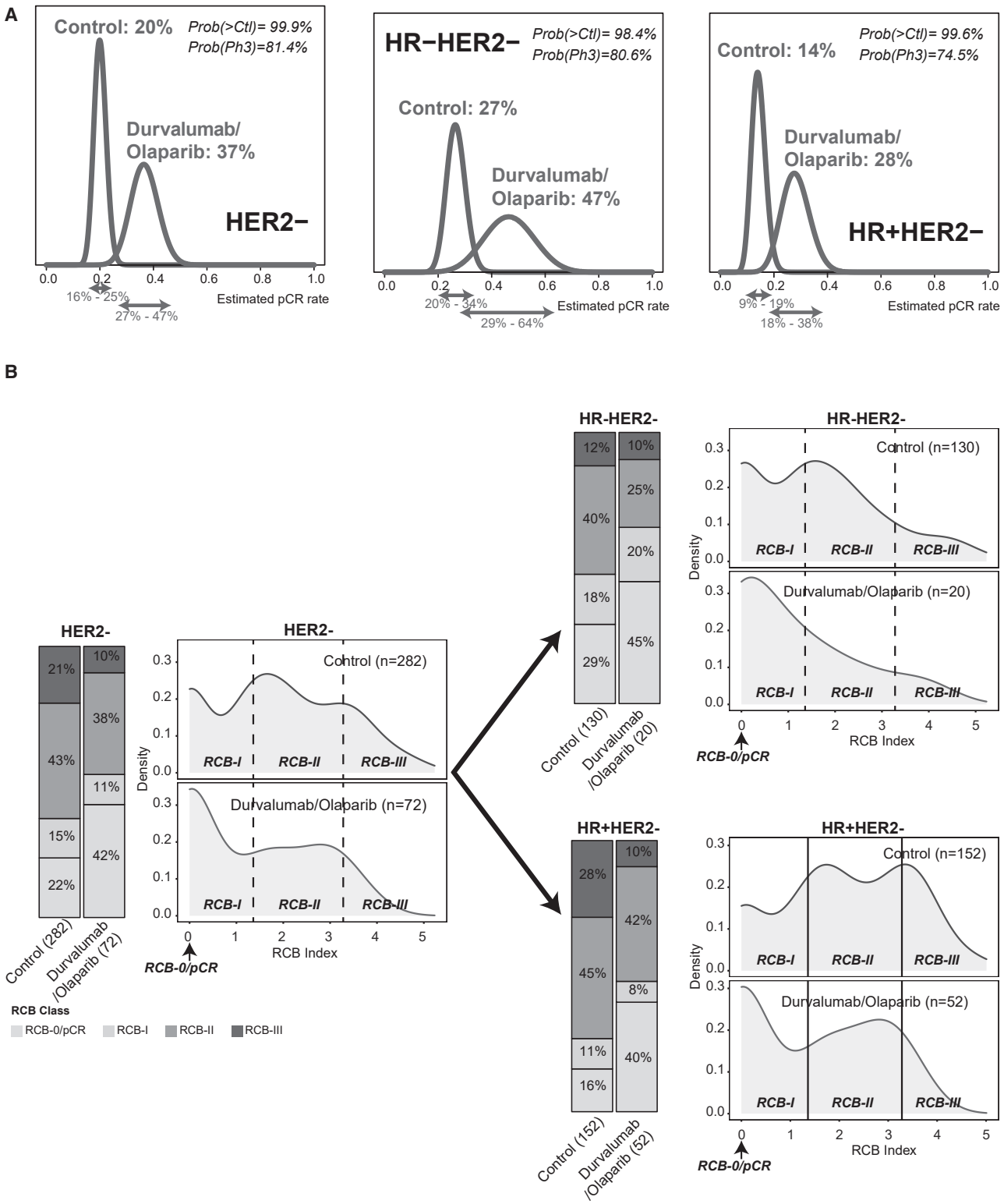

Figure 1. Bayesian probability distributions for achieving pathologic complete response and residual cancer burden distributions by treatment arm in the three *a priori* defined biomarker subsets

(A) Estimated pCR rates and the corresponding 95% probability intervals (x axes) for the experimental and control arms. Final predictive probabilities of success in a future 300 patient phase 3 trial (Prob(Ph3)), and the probabilities that the experimental arm is superior to the control (Prob(>Ctl)) are also shown.

(B) Residual cancer burden (RCB) categories and distribution of RCB scores by treatment arm in the three biomarker subsets.

Table 2. Grade 3 adverse events, dose reduction, and discontinuations rates

Adverse event	Agent (n = 73) Grade 1–2	Agent (n = 73) Grade 3–4	Control (n = 299) Grade 1–2	Control (n = 299) Grade 3–4
Neutropenia	10 (13.7%)	9 (12.3%)	17 (5.7%)	27 (9%)
Febrile neutropenia	0 (0%)	7 (9.6%)	0 (0%)	21 (7%)
Fatigue	63 (86.3%)	4 (5.5%)	202 (67.6%)	4 (1.3%)
Anemia	20 (27.4%)	3 (4.1%)	44 (14.7%)	13 (4.3%)
Neuropathy	50 (68.5%)	3 (4.1%)	176 (58.9%)	6 (2%)
Diarrhea	43 (58.9%)	3 (4.1%)	97 (32.4%)	4 (1.3%)
Adrenal insufficiency	1 (1.4%)	3 (4.1%)	0 (0%)	0 (0%)
White blood cell count decreased	8 (11%)	2 (2.7%)	14 (4.7%)	9 (3%)
Hypertension	6 (8.2%)	2 (2.7%)	36 (12%)	6 (2%)
Alanine aminotransferase increased	11 (15.1%)	2 (2.7%)	26 (8.7%)	4 (1.3%)
Stomatitis	27 (37%)	2 (2.7%)	77 (25.8%)	3 (1%)
Dehydration	5 (6.8%)	2 (2.7%)	13 (4.3%)	2 (0.7%)
Dyspnoea	19 (26%)	2 (2.7%)	46 (15.4%)	1 (0.3%)
Rash maculo-papular	13 (17.8%)	2 (2.7%)	48 (16.1%)	0 (0%)
Vaginal infection	3 (4.1%)	2 (2.7%)	4 (1.3%)	0 (0%)
Headache	31 (42.5%)	1 (1.4%)	88 (29.4%)	3 (1%)
Abdominal pain	23 (31.5%)	1 (1.4%)	33 (11%)	2 (0.7%)
Aspartate aminotransferase increased	10 (13.7%)	1 (1.4%)	19 (6.4%)	2 (0.7%)
Back pain	21 (28.8%)	1 (1.4%)	40 (13.4%)	2 (0.7%)
Nausea	53 (72.6%)	1 (1.4%)	176 (58.9%)	1 (0.3%)
Non-cardiac chest pain	4 (5.5%)	1 (1.4%)	14 (4.7%)	1 (0.3%)
Hypokalemia	5 (6.8%)	0 (0%)	14 (4.7%)	8 (2.7%)
Arthralgia/myalgia	46 (63%)	0 (0%)	149 (49.8%)	5 (1.7%)
Hyperglycemia	5 (6.8%)	0 (0%)	9 (3%)	3 (1%)
Pneumonitis	4 (5.5%)	0 (0%)	2 (0.7%)	2 (0.7%)
Vomiting	28 (38.4%)	0 (0%)	50 (16.7%)	2 (0.7%)
Onychalgia	3 (4.1%)	0 (0%)	17 (5.7%)	1 (0.3%)
Pruritus	11 (15.1%)	0 (0%)	32 (10.7%)	1 (0.3%)
Pyrexia	23 (31.5%)	0 (0%)	36 (12%)	1 (0.3%)
Urinary tract infection	4 (5.5%)	0 (0%)	11 (3.7%)	1 (0.3%)
Dose reductions	10 (13.7%)		23 (7.7%)	
Early discontinuation				
All	19 (26)		90 (30%)	
Toxicity	9 (12%)		20 (7%)	
Progression/lack of response	0 (0%)		33 (11%)	
Other	10 (14%)		37 (12%)	
Time from treatment consent to surgery (days)				
Median (range)	168 (107–273)		165 (85–289)	

Grade 3 adverse events reported during the entire treatment period (durvalumab/olaparib/paclitaxel [DOP] followed by doxorubicin/cyclophosphamide [AC] for the investigational arm and paclitaxel followed by AC for the control arm) are shown. Dose reductions and discontinuations are shown by treatment period.

lower SET expression, but there was no significant difference in the tumor inflammation signature (Figures 3C–3E). We also found that PARPi7 gene signature was significantly higher in the MP2 than in the MP1 group (likelihood ratio test p = 0.007). However, the PARPi7 signature correlated strongly with proliferation. The mRNA expression levels of BRCA1 and BRCA2 genes were not significantly associated with MP status.

DISCUSSION

Durvalumab and olaparib improved pCR rates when added to standard of care neoadjuvant chemotherapy from 20% to 37% in HER2-negative cancers. In TNBC, pCR rate improved from 27% to 47%; and in HR-positive/HER2-negative disease from 14% to 28%. Importantly, as indicated by RCB distributions,

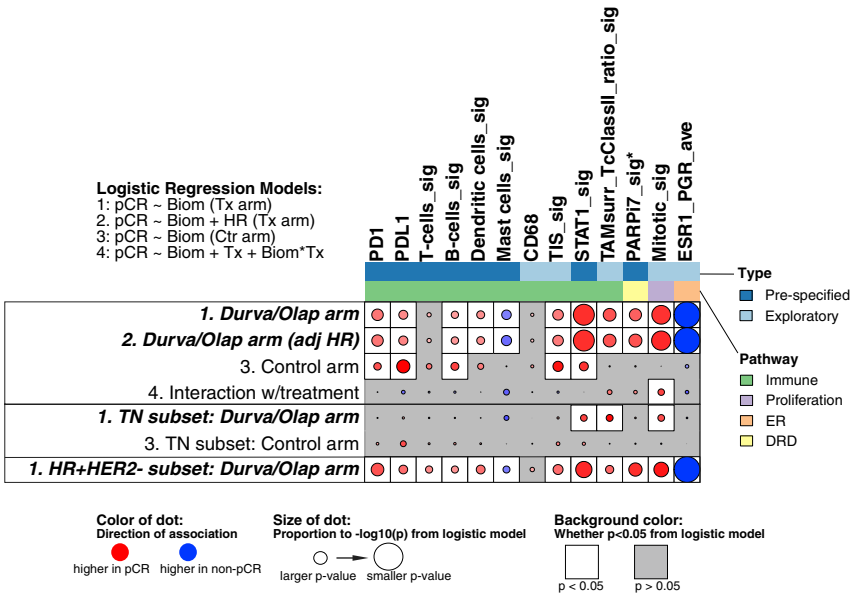

Figure 2. Predictive function of 13 mRNA markers in all HER2-negative, triple-negative cancers, and HER2-negative/hormone receptor-positive cancers

Red dots indicate a positive association with pCR, blue indicates association with residual disease. The size of the dots is inversely proportional to the p values; statistically significant associations are highlighted by the white rectangles. p values and associations were derived from logistic regression models as indicated by the numbers (1 through 4) on the figure.

even among patients who did not achieve pCR, the immune checkpoint inhibitor/PARP inhibitor combination reduced the amount of residual cancer across the entire spectrum of RCB scores in all HER2-negative subtypes.

We recognize that the pCR rates in I-SPY, particularly in the TNBC subset, are lower, 27%, than reported by other trials using taxane/anthracycline neoadjuvant chemotherapy (35%–40%). We believe that this is largely attributable to patients switching to non-protocol therapy, prompted by no-response/stable disease on imaging at 3 and 12 weeks, 11% of patients in the control arm discontinued early due to "progression/lack of sufficient response"; these patients are considered non-pCR per protocol, yet some end up with pCR at the time of surgery. From larger randomized trials (CALGB 40603, GeparSixto, GeparQuinto), that did not routinely assess response with imaging during therapy, we know that clinical progression on taxane/anthracycline regimens is <5%. Early imaging is integral to I-SPY, but it also turned out to be a liability because we lose patients who are concerned about lack of imaging response early on during treatment.

Two other trials evaluated the addition of durvalumab to neoadjuvant chemotherapy in TNBC. A single-arm phase I/II trial at Yale Cancer Center assessed durvalumab (10 mg/kg every 2 weeks) administered concurrently with weekly paclitaxel (80 mg/m^2) and dose-dense AC and reported a 44% pCR rate (Foldi et al., 2021). The randomized, GeparNuevo, phase II trial compared durvalumab (1,500 mg every 4 weeks) concurrent with weekly nab-paclitaxel and epirubicin/cyclophosphamide to the same chemotherapy alone and demonstrated a numerical, but not statistically significant increase in pCR rate from 44% to 53% (p = 0.287) (Loibl et al., 2019). The 95% confidence intervals of the pCR estimates in the experimental arms of these three trials 47% (95% CI: 29%–64%) in I-SPY2, 44% (95% CI: 30%–57%) in Yale phase I/II, and 53% (95% CI: 42%–61%) in GeparNuevo, respectively, overlap substantially despite the differences in durvalumab administration, chemotherapy back bones, and having a third drug, olaparib, in the I-SPY2 trial. Synergy between sequential taxane/platinum anthracycline neoadjuvant chemotherapy and PARP inhibitors was examined in two large neoadjuvant trials (BrighTNess, GeparOla), and both failed to demonstrate improved pCR rate with the addition of a PARP inhibitor in either germline *BRCA* mutant or wild-type breast cancers (Pusztai et al., 2020). Clinical trial data also remain inconclusive about the synergy between PARP inhibitors and immune checkpoint inhibitors (Peyraud and Italiano, 2020). Both the MEDIOLA (durvalumab + olaparib) and TOPACIO (niraparib + pembrolizumab) basket trials reported efficacy mostly in germline *BRCA* mutant cancers, where PARP inhibitors alone are expected to be effective. Overall, these results, suggest relatively modest, if any, contribution from olaparib to the increased pCR rate in the experimental arm of I-SPY2.

The DOP arm of I-SPY2 is the fourth randomized trial to demonstrate improvement in pCR rate with the inclusion of an immune checkpoint inhibitor in neoadjuvant chemotherapy for TNBC. A previously reported arm of I-SPY2 randomized patients to four cycles of pembrolizumab with weekly paclitaxel followed by AC (without pembrolizumab) and reported an increase in pCR from 22% to 60% (Nanda et al., 2020). This finding was confirmed in a large randomized trial, KN-522, that administered pembrolizumab concurrent with paclitaxel plus carboplatin followed by anthracycline/cyclophosphamide also with pembrolizumab and demonstrated a statistically significant increase in pCR from 51% to 65% (p = 0.0005) (Schmid et al., 2020). The recently presented Impassion-031 study also showed that atezolizumab in combination with albumin-bound paclitaxel followed by AC improved pCR rates (41% versus 58%, p = 0.004) compared with the same chemotherapy alone in TNBC (Miles et al., 2020). There are less data on the efficacy of neoadjuvant immune checkpoint therapy in HR-positive cancers. The only published result from a randomized trial is from the HR-positive/HER-negative cohort in the pembrolizumab arm of I-SPY2 that demonstrated improvement in pCR rate from 13% to 30% (Nanda et al., 2020), which is very similar to our current result showing that DOP increased the pCR rate from 14% to 28%.

In this, and all previously reported neoadjuvant trials, no unexpected safety signals, or perioperative complications were seen. However, there was an increase in known, immune-related adverse events in the experimental arms. The most common was thyroid function abnormalities. In this study 27.3% of

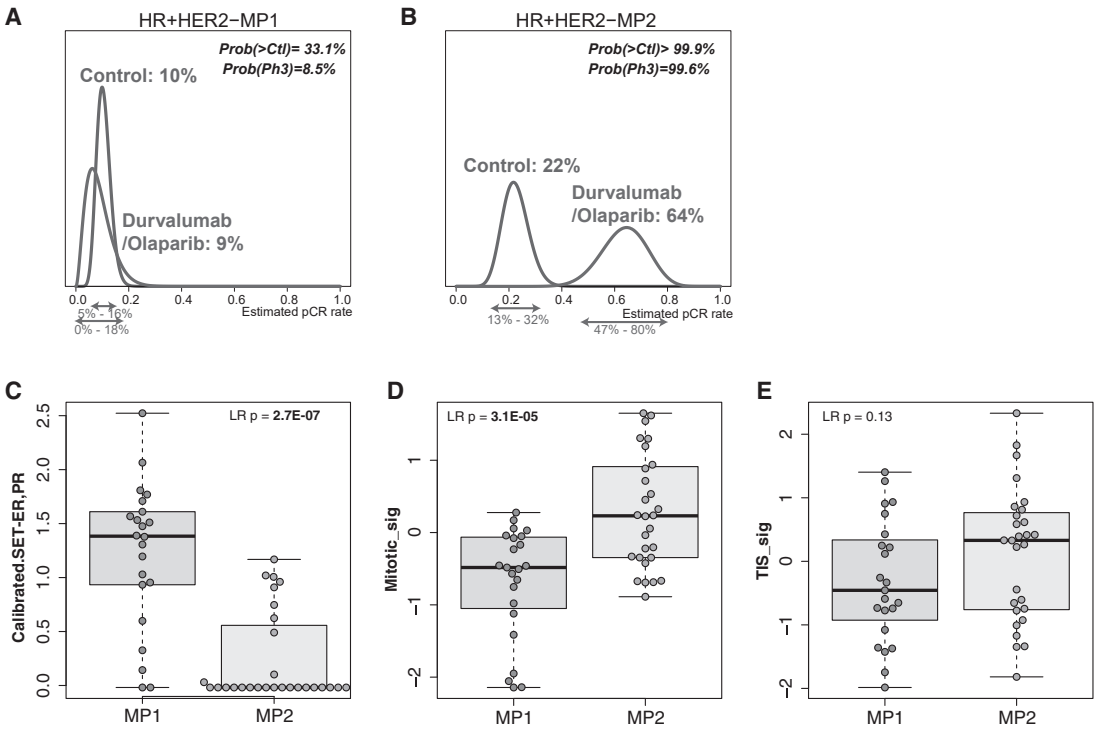

Figure 3. Bayesian probability distribution of pCR, and expression of proliferation, tumor inflammation, and SET gene signatures in MP1 and MP2 ER+/HER2– cancers

Estimated pCR rates and the corresponding 95% probability intervals (x axes) for the experimental and control arms in MP1 (A) and MP2 (B) cancers. Final predictive probabilities of success in a future 300 patient phase 3 trial (Prob(Ph3)), and the probabilities that the experimental arm is superior to the control (Prob(>Ctl)) are also shown. Expression of the sensitivity to endocrine therapy (SET) gene signature (C), and proliferation (D), and tumor inflammation (E) signatures in MP1 and MP2 cancers.

patients in the experimental arm experienced some immune-related adverse events, and 12.3% had a grade 3 or greater event, a rate very similar to that reported by the KN-522 trial using pembrolizumab.

Despite extensive efforts, it has been difficult to identify predictive biomarkers that identify stage II/III TNBC that selectively benefit from inclusion of immune checkpoint therapy with neoadjuvant chemotherapy. High tumor-infiltrating lymphocyte count, high expression of PD-L1 protein, and a broad range of immune-related genes predict for higher pCR rate with both chemotherapy alone and with chemotherapy plus immune checkpoint therapy (Miles et al., 2020; Gianni et al., 2020; Loibl et al., 2019; Schmid et al., 2020). Unlike in metastatic TNBC, in all neoadjuvant randomized trials, PD-L1 protein or mRNA expression did not define the population that selectively benefit from immune checkpoint therapy. We also observed that most immune signatures were positively associated with pCR in both treatment arms. At the individual marker level, some associations reached significance in the experimental arm but not the control arm; however, given the small and unequal cohort sizes and multiple tests, it is unclear if these are truly differentially predictive of response. In formal statistical testing, none of the immune markers showed significant marker-treatment interaction in TNBC.

HR-positive/HER2-negative patients with MammaPrint classified as "ultra-high" (MP2) showed selective benefit from durvalumab/olaparib. In MP2 patients, the pCR rate was 64% in the experimental arm compared with 22% in control; no benefit from the combination was seen in the MP1 group (pCR 9% versus 10%). Previously, we reported that MP2 status was significantly associated with pCR in HR-positive/HER2-negative patients randomized to the pembrolizumab arm of I-SPY (Yau et al., 2018). We also reported that the HR-positive/HER2-negative MP2 group benefited from adding carboplatin and veliparib to paclitaxel in an earlier arm of I-SPY2, where pCR rates were 33% versus 18%, whereas no improvement in pCR was seen in the MP1 group (Rugo et al., 2016). These findings suggest that the MP2 tumors are more chemotherapy sensitive than MP1 and this sensitivity is further enhanced by adding an immune checkpoint inhibitor. The molecular characteristics of the MP2 group, showing high proliferation and low ER and ER-related gene expression are consistent with greater chemotherapy sensitivity and lower endocrine therapy sensitivity of these cancers. These features also suggest that this subset of HR-positive cancers might derive substantial survival benefit from more effective chemotherapy that induces higher pCR. Benefit from adjuvant endocrine therapy, that could improve outcome in cases with residual cancer, is likely small in this subset due to low level of ER expression.

In conclusion, durvalumab and olaparib concurrent with weekly paclitaxel significantly improved pCR rate in all HER2-negative cancers, including TNBC and HR-positive cancers. Among the HR-positive/HER2-negative cancers, only the highly

proliferative, ER low, MammaPrint MP2 subset benefited from the combination therapy.

STAR★METHODS

Detailed methods are provided in the online version of this paper and include the following:

- KEY RESOURCES TABLE
- RESOURCE AVAILABILITY
  - Lead Contact
  - Materials availability
  - Data and code availability
- EXPERIMENTAL MODEL AND SUBJECT DETAILS
  - I-SPY 2 TRIAL Overview
  - Trial design
  - Eligibility
  - Treatment
  - Trial oversight
- METHOD DETAILS
  - Pretreatment biopsy processing and gene expression profiling
  - Biomarker analysis cohort definition
  - Continuous Gene Expression Biomarkers Assessed
  - Continuous gene expression biomarkers
  - *FFPE-revised PARPi-7 signature
  - MP1 and MP2 categorization
  - SET index
- QUANTIFICATION AND STATISTICAL ANALYSIS
  - I-SPY 2 efficacy analysis
  - The core bayesian logistic regression model
  - Adjusting for time trends
  - Time adjusted model (time machine)
  - Biomarker analysis

SUPPLEMENTAL INFORMATION

Supplemental information can be found online at https://doi.org/10.1016/j.ccell.2021.05.009.

ACKNOWLEDGMENTS

Supported by Quantum Leap Healthcare Collaborative (2013 to present) and the Foundation for the National Institutes of Health (2010–2012), a grant from the Gateway for Cancer Research (G-16-900), and by a grant (28XS197) from the National Cancer Institute Center for Biomedical Informatics and Information Technology. The authors sincerely appreciate the ongoing support for the I-SPY2 TRIAL from the Safeway Foundation, the William K. Bowes, Jr. Foundation, and Give Breast Cancer the Boot. Initial support was provided by Quintiles Transnational Corporation, Johnson & Johnson, Genentech, Amgen, the San Francisco Foundation, Eli Lilly, Pfizer, Eisai, Side Out Foundation, Harlan Family, the Avon Foundation for Women, Alexandria Real Estate Equities, and private individuals and family foundations.

We thank Anna Barker for leadership in helping to launch the I-SPY2 trial, the members of the data and safety monitoring committee, the trial coordinators, Ken Buetow and the staff of caBIG for input with the informatics design, the entire project oversight committee and the many investigators who have contributed. We are grateful for the input of our wonderful patient advocates: Susie Brain, Thelma Brown, Elly Cohen, Deborah Collyar, Coleen Crespo, Amy Delson, Peggy Devine, Sandra Finestone, Elizabeth Frank, Diane Heditsian, Patricia Haugen, Deborah Laxague, Marisa Leonardelli, Barbara LeStage, Beverly Parker, Susan Samson, and Patty Spears. Thank you to all the patients who volunteered to participate in I-SPY2.

AUTHOR CONTRIBUTIONS

All authors have reviewed the data analyses, contributed to data interpretation, contributed to the intellectual content of the manuscript, approved the final version to be published, and agree to be accountable for all aspects of the work. Conceptualization: L.J.E., D.A.B., A.M.D., N.M.H., L.J.v.V., D.Y., W.F.S., and J.P.; methodology: L.J.E., D.A.B., L.J.v.V., C.Y., D.M.W., L.P., H.S.H., L.D., L.S., E.F.P., J.D.W., M.C., and S.B.; formal analysis: C.Y., D.M.W., L.P., A.S., S.B., and D.A.B.; investigation: L.P., C.Y., D.M.W., H.S.H., L.D., A.M.W., E.S.-R., J.C.B., A.J.C., A.D.E., H.B., R.N., K.S.A., A.S.C., K. Kemmer, K. Kalinsky, C.I., A.T., R. Sanghrio, T.L.H., A.F.-T., M.C.L., L.B.-S., E.F.P., J.D.W., M.C., G.L.H., W.F.S., D.Y., L.J.v.V., N.M.H., A.M.D., and L.J.E.; data curation: C.Y., D.M.W., A.M.W., N.O., R. Sanghrio, A.S., A.L.A.; original draft: L.P., C.Y., D.M.W., H.S.H., R.N., D.Y., and J.B.M.; visualization: L.P., C.Y., B.Y., D.M.W., L.D., and A.S.; supervision: L.J.E., D.A.B., A.M.D., N.M.H., L.J.v.V., D.Y., W.F.S.,R. Sanghrio, H.S.R., M.M., L.P., and H.S.H.; project administration: S.M.A., R. Sanghrio, L.S., G.L.H., A.L.A., and J.B.M.; funding acquisition: L.J.E. and J.B.M.

DECLARATION OF INTERESTS

L. Pusztai has received consulting fees and honoraria from Pfizer, AstraZeneca, Merck, Novartis, Bristol-Myers Squibb Genentech, Eisai, Pieris, Immunomedics, Seattle Genetics, Clovis, Syndax, H3Bio, and Daiichi, and Nanostring research support to his institution from AstraZeneca, Pfizer, Merck, Seagen, and Bristol Myers Squibb.

H.S. Han: research funding to institution from GlaxoSmithKline, Abbvie, Prescient, G1 Therapeutics, Marker Therapeutics, Novartis, Horizon Pharma, Quantum Leap Healthcare Collaborative, Pfizer, Seattle Genetics, Arvinas, Zymeworks; grants from the Department of Defense, Speaker's Bureau - Lilly.

E. String-Reasor: Consulting Lilly; Susan G. Komen, BCRFA, V Foundation research funding.

J.C. Boughey: research funding from Eli Lilly.

A.J. Chien: institutional research funding from Seagen, Merck, Amgen, and Puma.

R. Nanda: research funding from Arvinas, AstraZeneca, Celgene, Corcept Therapeutics, Genentech/Roche, Immunomedics/Gilead, Merck, OBI Pharm, Inc., Odonate Therapeutics, OncoSec, Pfizer, Taiho, SeaGen.

A.S. Clark: research funding from Novartis.

K. Kalinsky has disclosed advisory/consulting funding from Eli-Lilly, Pfizer, Novartis, Eisai, AstraZeneca, Immunomedics, Merck, Seattle Genetics, OncoSec, 4D Pharma, DaicchiSankyo, and Cyclocel. Dr. Kalinsky also reports financial disclosures for his spouse (stock): Grail, Array BioPharma and Pfizer (prior employee).

C. Isaacs has received consulting fees from Seattle Genetics, Genentech, AstraZeneca, Novartis, PUMA, Pfizer, and Esai.

A. Thomas declares research support (paid to the institution) from Seattle Genetics, Sanofi; stock ownership in Johnson and Johnson, Bristol Myers Squibb, Pfizer, and Gilead; and participation in DSMB (BeyondSpring Pharmaceuticals; and royalties from Up-to-Date).

A. Forero-Torres became a Seattle Genetics employee in 2018, and holds stock option from this employment.

M.C. Liu received clinical trial research support from Eisai, Genentech, GRAIL, Menarini Silicon Biosystems, Merck, Novartis, Seattle Genetics, and Tesaro.

M. Melisko received research funding to the institution from AstraZeneca, Novartis, KCRN Research, and Puma, and consulting fees from Biotheranostics, their spouse received honoraria from Genentech and has stock ownership in Merrimack.

E.F. Petricoin: leadership roles in Perthera, Ceres Nanosciences; stock and other ownership interests in Perthera, Ceres Nanosciences, Avant Diagnostics; consulting or advisory roles in Perthera, Ceres Nanosciences, AZGen, Avant Diagnostics; research funding from Ceres Nanosciences (Inst), GlaxoSmithKline (Inst), Abbvie (Inst), Symphogen (Inst), Genentech (Inst); patents, royalties, other intellectual property (National Institutes of Health patents licensing fee distribution/royalty; co-inventor on filed George Mason University–assigned patents related to phosphorylated HER2 and EGFR response predictors for HER family-directed therapeutics, as such can receive

CellPress

royalties and licensing distribution on any licensed IP; travel, accommodations, and expenses from Perthera, Ceres Nanosciences.

J.D. Wulfkuhle received honoraria from DAVA Oncology and consults for Baylor College of Medicine, and has disclosed stock ownership in Theralink Technologies, Inc.

H.S. Rugo has received research support for clinical trials through the University of California from Pfizer, Merck, Novartis, Lilly, Genentech, Odonate, Daiichi, Seattle Genetics, Eisai, Macrogenics, Sermonix, Boehringer Ingelheim, Polyphor, AstraZeneca, and Immunomedics; and Honoraria from Puma, Mylan, and Samsung.

L.J. van't Veer is employed by and a stockholder of Agendia NV.

L.J. Esserman is an unpaid member of the board of directors of Quantum Leap Healthcare Collaborative, and received grant funding from QLHC for the I-SPY TRIAL; and is a member of the Blue Cross/Blue Shield Medical Advisory Panel and receives reimbursement for her time and travel. She has a grant from Merck for an Investigator initiated trial of DCIS.

The following authors declare no competing interests: C.Y., D.M.W., L.D., A.M.W., A.D., E.H.B., K.S.A., R. Shatsky, L.S., S.M.A., A.W., R. Singhrao, L.S., G.L.H., S.M.B., A.A., J.P., R.B.S., D.Y., N.M.H., K. Kemmer, T.L.H., A.S., J.B.M., W.F.S., A.M.D., and D.A.B.

INCLUSION AND DIVERSITY

We worked to ensure gender balance in the recruitment of human subjects. We worked to ensure ethnic or other types of diversity in the recruitment of human subjects. We worked to ensure that the study questionnaires were prepared in an inclusive way. One or more of the authors of this paper self-identifies as an underrepresented ethnic minority in science. While citing references scientifically relevant for this work, we also actively worked to promote gender balance in our reference list. The author list of this paper includes contributors from the location where the research was conducted who participated in the data collection, design, analysis, and/or interpretation of the work.

ROLE OF FUNDING SOURCE

The trial was designed by the I-SPY2 study investigators. AstraZeneca provided the study drug and funding, but played no role in the study design, collection/analysis of data, or in manuscript preparation. The I-SPY2 trial is sponsored by Quantum Leap Healthcare Collaborative (2013 to present) and the Foundation for the National Institutes of Health (2010 to 2012) and by a grant (28XS197) from the National Cancer Institute Center for Biomedical Informatics and Information Technology. The authors of the manuscript vouch for the accuracy and completeness of the data.

Received: December 7, 2020
Revised: March 1, 2021
Accepted: May 17, 2021
Published: June 17, 2021

REFERENCES

Ayers, M., Lunceford, J., Nebozhyn, M., Murphy, E., Loboda, A., Kaufman, D.R., Albright, A., Cheng, J.D., Kang, S.P., Shankaran, V., et al. (2017). IFN-γ-related mRNA profile predicts clinical response to PD-1 blockade. J. Clin. Invest. *127*, 2930–2940.

Barker, A., Sigman, C., Kelloff, G., Hylton, N., Berry, D., and Esserman, L. (2009). I-SPY 2: an adaptive breast cancer trial design in the setting of neoadjuvant chemotherapy. Clin. Pharmacol. Ther. *86*, 97–100.

Berry, D.A. (2011). Adaptive clinical trials in oncology. Nat. Rev. Clin. Oncol. *9*, 199–207.

Berry, S.M., Reese, C.S., and Larkey, P.D. (2012). Bridging different eras in sports. J. Am. Stat. Assoc. *94*, 661–676.

Bianchini, G., Pusztai, L., Karn, T., Iwamoto, T., Rody, A., Kelly, C.M., Müller, V., Schmidt, M., Qi, Y., Holtrich, U., et al. (2013). Proliferation and estrogen signaling can distinguish patients at risk for early versus late relapse among estrogen receptor positive breast cancers. Breast Cancer Res. *15*, R86.

Campbell, M.J., Wolf, D., Mukhtar, R.A., Tandon, V., Yau, C., Au, A., Baehner, F., van't Veer, L., Berry, D., and Esserman, L.J. (2013). The prognostic implications of macrophages expressing proliferating cell nuclear antigen in breast cancer depend on immune context. PLoS One *8*, e79114.

Cardoso, F., van't Veer, L.J., Bogaerts, J., Slaets, L., Viale, G., Delaloge, S., Pierga, J.-Y., Brain, E., Causeret, S., DeLorenzi, M., et al. (2016). 70-Gene signature as an aid to treatment decisions in early-stage breast cancer. New Engl. J. Med. *375*, 717–729.

Daemen, A., Wolf, D.M., Korkola, J.E., Griffith, O.L., Frankum, J.R., Brough, R., Jakkula, L.R., Wang, N.J., Natrajan, R., Reis-Filho, J.S., et al. (2012). Cross-platform pathway-based analysis identifies markers of response to the PARP inhibitor olaparib. Breast Cancer Res. Treat. *135*, 505–517.

Danaher, P., Warren, S., Dennis, L., D'Amico, L., White, A., Disis, M.L., Geller, M.A., Odunsi, K., Beechem, J., and Fling, S.P. (2017). Gene expression markers of tumor infiltrating leukocytes. J. Immunother. Cancer *5*, 18.

Domchek, S.M., Postel-Vinay, S., Im, S.-A., Park, Y.H., Delord, J.-P., Italiano, A., Alexandre, J., You, B., Bastian, S., Krebs, M.G., et al. (2020). Olaparib and durvalumab in patients with germline BRCA-mutated metastatic breast cancer (MEDIOLA): an open-label, multicentre, phase 1/2, basket study. Lancet Oncol. *21*, 1155–1164.

Esteva, F.J., Hubbard-Lucey, V.M., Tang, J., and Pusztai, L. (2019). Immunotherapy and targeted therapy combinations in metastatic breast cancer. Lancet Oncol. *20*, e175–e186.

Foldi, J., Silber, A., Reisenbichler, E., Singh, K., Fischbach, N., Persico, J., Adelson, K., Katoch, A., Horowitz, N., Lannin, D., et al. (2021). Neoadjuvant durvalumab plus weekly nab-paclitaxel and dose-dense doxorubicin/cyclophosphamide in triple-negative breast cancer. Npj Breast Cancer *7*, 9.

Gianni, L., Huang, C.-S., Egle, D., Bermejo, B., Zamagni, C., Thill, M., Anton, A., Zambelli, S., Bianchini, G., Russo, S., et al. (2020). Abstract GS3-04: pathologic complete response (pCR) to neoadjuvant treatment with or without atezolizumab in triple negative, early high-risk and locally advanced breast cancer. NeoTRIPaPDL1 Michelangelo randomized study. Cancer Res. *80*, GS3-04-GS3-04.

Lassen, U. (2019). Combining PARP inhibition with PD-1 inhibitors. Lancet Oncol. *20*, 1196–1198.

Loibl, S., Untch, M., Burchardi, N., Huober, J., Sinn, B.V., Blohmer, J.U., Grischke, E.M., Furlanetto, J., Tesch, H., Hanusch, C., et al. (2019). A randomised phase II study investigating durvalumab in addition to an anthracycline taxane-based neoadjuvant therapy in early triple-negative breast cancer: clinical results and biomarker analysis of GeparNuevo study. Ann. Oncol. *30*, 1279–1288.

Miles, D.W., Gligorov, J., André, F., Cameron, D., Schneeweiss, A., Barrios, C.H., Xu, B., Wardley, A.M., Kaen, D., Andrade, L., et al. (2020). Primary results from IMpassion131, a double-blind placebo-controlled randomised phase III trial of first-line paclitaxel (PAC)±atezolizumab (atezo) for unresectable locally advanced/metastatic triple-negative breast cancer (mTNBC). Ann Onc *31*, S1147–S1148.

Nanda, R., Liu, M.C., Yau, C., Shatsky, R., Pusztai, L., Wallace, A., Chien, A.J., Forero-Torres, A., Ellis, E., Han, H., et al. (2020). Effect of pembrolizumab plus neoadjuvant chemotherapy on pathologic complete response in women with early-stage breast cancer: an analysis of the ongoing phase 2 adaptively randomized I-SPY2 trial. Jama Oncol. *6*, 676–684.

Oken, M.M., Creech, R.H., Tormey, D.C., Horton, J., Davis, T.E., McFadden, E.T., and Carbone, P.P. (1982). Toxicity and response criteria of the Eastern-Cooperative-Oncology-Group. Am. J. Clin. Oncol. *5*, 649–655.

Pantelidou, C., Sonzogni, O., Taveira, M.D.O., Mehta, A.K., Kothari, A., Wang, D., Visal, T., Li, M.K., Pinto, J., Castrillon, J.A., et al. (2019). PARP inhibitor efficacy depends on CD8+ T-cell recruitment via intratumoral STING pathway activation in BRCA-deficient models of triple-negative breast cancer. Cancer Discov. *9*, 722–737.

Park, J.W., Liu, M.C., Yee, D., Yau, C., van t Veer, L.J., Symmans, W.F., Paoloni, M., Perlmutter, J., Hylton, N.M., Hogarth, M., et al. (2016). Adaptive randomization of neratinib in early breast cancer. New Engl. J. Med. *375*, 11–22.

Peyraud, F., and Italiano, A. (2020). Combined PARP inhibition and immune checkpoint therapy in solid tumors. Cancers *12*, 1502.

Pusztai, L., Reisenbichler, E., Bai, Y., Fischbach, N., Persico, J., Adelson, K., Katoch, A., Horowitz, N., Lannin, D., Killelea, B., et al. (2020). Abstract PD1-01: durvalumab (MEDI4736) concurrent with nab-paclitaxel and dose dense doxorubicin cyclophosphamide (ddAC) as neoadjuvant therapy for triple negative breast cancer (TNBC). Cancer Res. *80*, PD1-01-PD1-01.

Rody, A., Holtrich, U., Pusztai, L., Liedtke, C., Gaetje, R., Ruckhaeberle, E., Solbach, C., Hanker, L., Ahr, A., Metzler, D., et al. (2009). T-cell metagene predicts a favorable prognosis in estrogen receptor-negative and HER2-positive breast cancers. Breast Cancer Res. *11*, R15.

Rugo, H.S., Olopade, O.I., DeMichele, A., Yau, C., van t Veer, L.J., Buxton, M.B., Hogarth, M., Hylton, N.M., Paoloni, M., Perlmutter, J., et al. (2016). Adaptive randomization of veliparib-carboplatin treatment in breast cancer. New Engl. J. Med. *375*, 23–34.

Schmid, P., Cortés, J., Pusztai, L., McArthur, H., Kümmel, S., Bergh, J., Denkert, C., Park, Y.H., Hui, R., Harbeck, N., et al. (2020). Pembrolizumab for early triple-negative breast cancer. New Engl. J. Med. *382*, 810–821.

Sinn, B.V., Fu, C., Lau, R., Litton, J., Tsai, T.-H., Murthy, R., Tam, A., Andreopoulou, E., Gong, Y., Murthy, R., et al. (2019). SETER/PR: a robust 18-gene predictor for sensitivity to endocrine therapy for metastatic breast cancer. Npj Breast Cancer *5*, 16.

Stewart, R., Morrow, M., Hammond, S.A., Mulgrew, K., Marcus, D., Poon, E., Watkins, A., Mullins, S., Chodorge, M., Andrews, J., et al. (2015). Identification and characterization of MEDI4736, an antagonistic anti–PD-L1 monoclonal antibody. Cancer Immunol. Res. *3*, 1052–1062.

Symmans, W.F., Hatzis, C., Sotiriou, C., André, F., Peintinger, F., Regitnig, P., Daxenbichler, G., Desmedt, C., Domont, J., Marth, C., et al. (2010). Genomic index of sensitivity to endocrine therapy for breast cancer. J. Clin. Oncol. *28*, 4111–4119.

Symmans, W.F., Wei, C., Gould, R., Yu, X., Zhang, Y., Liu, M., Walls, A., Bousamra, A., Ramineni, M., Sinn, B., et al. (2017). Long-term prognostic risk after neoadjuvant chemotherapy associated with residual cancer burden and breast cancer subtype. J. Clin. Oncol. *35*, 1049–1060.

West, M., and Harrison, J. (1997). Bayesian Forecasting and Dynamic Models (Springer).

Wolf, D.M., Yau, C., Sanil, A., Glas, A., Petricoin, E., Wulfkuhle, J., Severson, T.M., Linn, S., Brown-Swigart, L., Hirst, G., et al. (2017). DNA repair deficiency biomarkers and the 70-gene ultra-high risk signature as predictors of veliparib/carboplatin response in the I-SPY 2 breast cancer trial. Npj Breast Cancer *3*, 31.

Yau, C., Wolf, D., Brown-Swigart, L., Hirst, G., Sanil, A., Singhrao, R., Investigators, I.-S.2T., Asare, S., DeMichele, A., Berry, D., et al. (2018). Abstract PD6-14: analysis of DNA repair deficiency biomarkers as predictors of response to the PD1 inhibitor pembrolizumab: results from the neoadjuvant I-SPY 2 trial for stage II-III high-risk breast cancer. Cancer Res. *78*, PD6–14.

STAR★METHODS

KEY RESOURCES TABLE

REAGENT or RESOURCE	SOURCE	IDENTIFIER
Biological samples		
Tumor biopsy before treatment	I-SPY 2 TRIAL	https://clinicaltrials.gov/ct2/show/NCT01042379
Critical commercial assays		
Custom Agilent 44K expression arrays	Agendia, Inc	https://www.ncbi.nlm.nih.gov/geo/query/acc.cgi?acc=GPL20078
MammaPrint	Agendia, Inc	https://agendia.com/mammaprint/
Deposited data		
Raw and processed transcriptomic data	This study	GEO accession number: GSE173839 https://www.ncbi.nlm.nih.gov/geo/query/acc.cgi?acc=GSE173839
Patient-level expression signature and clinical data	This study	GEO accession number: GSE173839 https://www.ncbi.nlm.nih.gov/geo/query/acc.cgi?acc=GSE173839
Software and algorithms		
stats R package (v.3.6.3)	R Core Team (2020)	https://stat.ethz.ch/R-manual/R-devel/library/stats/html/stats-package.html
lmtest R package (v.0.9-37)	Zeileis A, Hothorn T (2002). "Diagnostic Checking in Regression Relationships." R News, 2(3), 7–10.	https://CRAN.R-project.org/package=lmtest
rjags R package (v.4-10)	Martyn Plummer (2019). rjags: Bayesian Graphical Models using MCMC. R package v4-10.	https://CRAN.R-project.org/package=rjags

RESOURCE AVAILABILITY

Lead Contact

Further information and requests for resources or data should be directed to the I-SPY Data Access and Publications Committee coordinator (ispy2dapc@quantumleaphealth.org).

Materials availability

Requests for sharing of materials should be directed to the lead contact.

Data and code availability

Transcriptomic and clinical data used in this study is available at https://www.ncbi.nlm.nih.gov/geo/query/acc.cgi?acc=GSE173839. Additional de-identified subject level data may be requested by qualified investigators. Details of the trial, data, contact information, proposal forms, and review and approval process are available at the following website: https://www.ISPYtrials.org/collaborate/proposal-submissions.

EXPERIMENTAL MODEL AND SUBJECT DETAILS

I-SPY 2 TRIAL Overview

I-SPY2 is an ongoing, open-label, adaptive, randomized phase II, multicenter trial of neoadjuvant therapy for early-stage breast cancer (NCT01042379). It is a platform trial evaluating multiple investigational arms in parallel against a common standard of care control arm. The primary endpoint is pCR (ypT0/is, ypN0), defined as the absence of invasive cancer in the breast and regional nodes at the time of surgery. As I-SPY2 is modified intent-to-treat, patients receiving any dose of study therapy are considered evaluable; those who switch to non-protocol therapy, progress, forgo surgery, or withdraw are deemed 'non-pCR'. Secondary endpoints include residual cancer burden (RCB) and event-free and distant relapse-free survival (EFS and DRFS) (Symmans et al., 2017).

Trial design

Assessments at screening establish eligibility and classify participants into subtypes defined by hormone receptor (HR) status, HER2, and 70-gene signature (Mammaprint) status (Cardoso et al., 2016) Adaptive randomization in I-SPY2 preferentially assigns patients to trial arms according to continuously updated Bayesian probabilities of pCR rates within each biomarker signature; 20% of patients are randomly assigned to the control arm(Berry, 2011). While accrual is ongoing, a statistical engine assesses the accumulating pathologic and MRI responses at weeks 3 and 12 and continuously re-estimates the probabilities of an experimental arm being superior to the control in each defined biomarker signature. An arm can be dropped for futility if the predicted probability of success in a future 300-patient, 1:1 randomized, phase 3 trial drops below 10%, or graduate for efficacy if the probability of success reaches 85% or greater in any biomarker signature. The clinical control arm for the efficacy analysis uses patients randomized throughout the entire trial. Experimental arms have variable sample sizes: highly effective therapies graduate with fewer patients in the experimental arm; arms that are equal to, or marginally better than, the control arm accrue slower and are stopped if they have not graduated, or terminated for lack of efficacy, before reaching a sample size of 75. During the design of each new experimental arm the investigators together with the pharmaceutical sponsor decide in which of the 10 a priori defined biomarker signatures the drug will be tested. Upon entry to the trial, participants are dichotomized into hormone receptor (HR) negative versus positive, HER2 positive versus negative, and MammaPrint High1 [MP1] versus High2 [MP2] status. From these 8 biomarker combinations (2 × 2 × 2) I-SPY has created 10 biomarker signatures that represent the disease subsets of interest (e.g. all patients, all HR+, all HER2+, HR+/HER2-, etc, for complete list see reference (Berry, 2011)) in which a drug can be tested for efficacy.

The DOP arm was studied in three subtypes including (i) all HER2-negative, (ii) TNBC, and (iii) HR positive/HER2-negative cancers. HER2 positive patients were not eligible for randomization into this arm. Efficacy is monitored in each of these biomarker signatures separately and an arm could graduate in any or all biomarker signature of interest. When graduation occurs, accrual to the arm stops, final efficacy results are updated when all pathology results are complete. The final estimated pCR results therefore may differ from the predicted pCR rate at the time of graduation. Additional details on the study design have been published elsewhere (Park et al., 2016; Rugo et al., 2016).

Eligibility

Participants eligible for I-SPY2 are women >18 years of age with stage II or III breast cancer with a minimum tumor size of >2·5 cm by clinical exam, or >2·0 cm by imaging, and Eastern Cooperative Oncology Group performance status of 0 or 1 (Oken et al., 1982). HR-positive/HER2-negative cancers assessed as low risk by the 70-gene MammaPrint test are ineligible as they receive little benefit from systemic chemotherapy. Only HER2-negative patients were eligible for randomization to the olaparib/durvalumab arm. Additional exclusion criteria for this arm included prior PARP inhibitor or immune checkpoint inhibitor therapy, use of immunosuppressive medications, or history of autoimmune disease.

Treatment

All HER2-negative participants in I-SPY2 receive standard of care neoadjuvant chemotherapy, which also served as the control arm, consisting of intravenous paclitaxel 80 mg/m^2 weekly for 12 weeks, followed by four cycles of 60 mg/m^2 doxorubicin and 600 mg/m^2 cyclophosphamide (AC) every 2-3 weeks. Participants in the experimental arm also received 3 cycles of intravenous durvalumab 1500 mg every 4 weeks and 100mg oral olaparib twice a day from weeks 1 through 11, concurrent with paclitaxel. For the first paclitaxel infusion, 20 mg dexamethasone was given and if no infusion reaction occurred, dexamethasone was reduced to 10 mg for week two, if no infusion reaction was observed with the first two treatments, dexamethasone was discontinued. Dose reductions and toxicity management were specified in the protocol. Adverse events were collected according to the NCI Common Terminology Criteria for Adverse Events (CTCAE) version 4.0.

After completion of AC, patients underwent lumpectomy or mastectomy and nodal sampling, with choice of surgery at the discretion of the treating surgeon. All patients were screened for potential adrenal insufficiency before surgery with a morning serum cortisol level.

Trial oversight

I-SPY2 is conducted in accordance with the guidelines for Good Clinical Practice and the Declaration of Helsinki, with approval for the study protocol and associated amendments obtained from independent ethics committees at each site. Written, informed consent was obtained from each participant prior to screening and again prior to treatment. The I-SPY2 Data Safety Monitoring Board meets monthly to review patient safety.

METHOD DETAILS

Pretreatment biopsy processing and gene expression profiling

Core needle biopsies of 16-gauge were taken from the primary breast tumor at screening, before treatment. I-SPY2 changed biopsy requirements from fresh frozen (FF) tissue to formalin fixed paraffin embedded (FFPE) tissues in May 2018; therefore, all DOP patients had RNA extracted from FFPE biopsies. The collected tissue samples are immediately placed in 10% Neutral Buffered Formalin for between 6 and 72 hr before dehydration and processing to FFPE blocks. A 5μM section is stained with hematoxylin and eosin (H&E) and pathologic evaluation performed to confirm the tissue contains at least 30% tumor. A tissue sample meeting the 30% or greater

tumor cellularity requirement is further sectioned centrally at the I-SPY 2 laboratory to produce between ten to thirty 5 μM sections collected on charged slides microarray profiling. The sections are processed at Agendia, Inc., for RNA extraction and gene expression profiling on Agilent 44K microarrays. For each array, the green channel mean signal is log2-tranformed and centered within array to its 75th quantile as per the manufacturer's data processing recommendations. A fixed value of 9.5 is added to avoid negative values.

Biomarker analysis cohort definition

For the first 7 years of the I-SPY 2 TRIAL, only fresh frozen tumor (FF) tissues were collected and assayed for gene expression using Agilent microarrays. In 2018, Agendia switched to analyzing only the FFPE samples. The DOP arm opened in 2018 and therefore these patients have FFPE-derived biomarker data. The clinical control arm for the DOP efficacy analysis used patients randomized throughout the entire trial. Therefore, samples that match to the clinical control arm include expression data derived from FF (n = 265) and FFPE (n = 34) tissues. During a pilot study of 74 patients where both FF and FFPE samples were assayed for mRNA expression to assess interchangeability of the tissue sources we noted that that for several of the immune gene signatures that we evaluated, the correlation coefficient ranged from 0.35 to 0.77. Because of the low concordance, we decided to only include the 34 FFPE-derived expression data from the control arm in the gene signature analysis to provide comparable results to the 71 samples from the DOP arm. The MammaPrint scores are required for I-SPY 2 trial eligibility that is performed with an FDA approved assay, and therefore, the MP 1 and MP1 class are available for all patients.

Continuous Gene Expression Biomarkers Assessed

Nine gene signatures were examined as predictors of response to durvalumab/olaparib, including a proliferation signature (mitotic score) (Bianchini et al., 2013), a DNA repair deficiency signature (PARPi7) (Daemen et al., 2012; Wolf et al., 2017), and 7 immune signatures corresponding to various immune cell types (Danaher et al., 2017) (T cell, B cell, dendritic cell, mast cell), STAT1 cytokine signaling (Rody et al., 2009), macrophage/T cell ratio (Campbell et al., 2013) and an immunotherapy response signature (Ayers et al., 2017) (tumor inflammatory signature). These gene signatures were taken from the literature and each has been associated with response to chemotherapy, targeted therapy, or prognosis. mRNA expression of single genes ESR1 (ER), PGR (PR), CD274 (PDL1), CD279 (PD1) and CD68 (macrophage marker) were also assessed.

Continuous gene expression biomarkers

Table S2 lists the 13 gene expression biomarkers evaluated as predictors of response to durvalumab/olaparib, along with their type (pre-specified or exploratory), pathway designation, member genes, implementation method, and PubMed ID of references.

*FFPE-revised PARPi-7 signature

The PARPi-7 DNA repair deficiency signature as published was developed and tested on gene expression data from fresh frozen (FF) samples (Daemen et al., 2012; Wolf et al., 2017). As PARPi-7 contains genes that are not highly correlated across FF and FFPE, we replaced poorly translating genes by others in the same DNA repair pathway that (1) correlate to the original genes in FF, (2) associate with response to veliparib/carboplatin, and (3) are correlated in expression data generated from FF and FFPE tissues. We evaluated this revisedPARPi-7 by 1) extracting revised predictor genes BRCA1 (A_23_P207400), CHEK2 (A_23_P109452), MAPKAPK2 (A_23_P201483), XRCC4 (A_23_P122174), RAD17 (A_24_P97836), POLB (A_32_P34552), and CIRBP (AG_0673); 2) combining probesets for normalization genes RPL24, ABI2, GGA1, E2F4, IPO8, CXXC1, and RPS10 into gene level summaries by averaging; 3) dividing each PARPi-7 predictor gene level by the geometric mean of the normalization genes; 4) log2-transforming each ratio and median centering across the population; and 5) calculating signature scores using the published weights and boundaries: Weights < -c(-0.5320, 0.5806, 0.0713, −0.1396, −0.1976, - 0.3937, −0.2335), Boundaries < -c(-0
.0153, −0.006, 0.0031, −0.0044, 0.0014, −0.0165, −0.0126), Score = Weights*(Genes -Boundaries). The score is then standardized to sd = 1; and used for our qualifying biomarker evaluation.

MP1 and MP2 categorization

In I-SPY2, patients were classified as Mammaprint High risk (MP1) or Mammaprint ultra-high risk (MP2) by Agendia, Inc., using a predefined threshold applied to the MP 70-gene risk score evaluated on Agilent 44K arrays. The threshold used is equivalent to the median cut point of I-SPY 1 participants (−0.154 in the original ISPY 1 dataset) who fit the eligibility criteria for I-SPY 2.

SET index

The 'sensitivity to endocrine therapy' ($SET_{ER/PR}$) gene signature includes the ESR1 gene and 17 other estrogen (ER) and progesterone (PR) receptor regulated transcripts(Sinn et al., 2019). The $SET_{ER/PR}$ signature is predictive of progression-free and overall survival in both metastatic and early-stage HR-positive breast cancers treated with endocrine therapy(Sinn et al., 2019; Symmans et al., 2010). We evaluated the distribution of the SET index in the MP1 and MP2 subtypes of the HR-positive/HER2-negative cohort. All HR-positive patients included in I-SPY2 are Mammaprint high, but these patients can be further subdivided into high risk (MP1) and ultra-high risk (MP2) groups as described above and as published previously.

QUANTIFICATION AND STATISTICAL ANALYSIS

I-SPY 2 efficacy analysis

The I-SPY 2 efficacy analysis model have two main components: (1) a core covariate-adjusted Bayesian logistic regression and (2) an adjustment for time trends as described below.

The core bayesian logistic regression model

Probability distributions of pCR are calculated using a Bayesian covariate-adjusted logistic model with HR, HER2 and MammaPrint statuses as covariates for each eligible si

gnature. Let $y_i \in \{0,1\}$ be the indicator for the pCR response of patient i $(i = 1,\ldots,N)$. Covariates $x_{1i}, x_{2i}, x_{3i} \in \{0,1\}$ represent the HR, HER2 and MP statuses of patient i (with 1 indicating positive and 0 negative for HR and HER2 and 'High1' and 'High2' for MP). Label A_i the treatment arm assigned to patient i.

The model is

$$y_i \sim Bernoulli(p_i)$$

$$logit(p_i) = \beta_0 + \beta_1 x_{1i} + \beta_2 x_{2i} + \beta_3 x_{3i} + \theta_{A_i} + \gamma_{1,A_i} x_{1i} + \gamma_{2,A_i} x_{2i} + \gamma_{3,A_i} x_{3i}$$

The model's components are as follows:

- The $\beta_1 x_{1i} + \beta_2 x_{2i} + \beta_3 x_{3i}$ terms capture the effect of being in a particular subtype defined by (HR, HER2, MP) status.
- The $\gamma_{1,A_i} x_{1i}$, $\gamma_{2,A_i} x_{2i}$, $\gamma_{3,A_i} x_{3i}$ terms are the treatment effects within each of the (HR, HER2, MP) subtype.
- We set $\theta_0 = \gamma_{1,0} = \gamma_{2,0} = \gamma_{3,0} = 0$ to ensure parameter identifiability.
- The θ_{A_i} represent the effect of being on a particular treatment arm for all patients.

For each of the coefficients Θ in the regression model, we assume independent normal prior distributions: $\Theta \sim N(\mu_\Theta, \sigma^2_\Theta) = N(0,1)$.

We also include the data from the control arm of the I-SPY 1 trial as historical prior information. However, the likelihood function evaluation corresponding to the I-SPY1 data is raised to the power of 0.2 to reflect a discounting or weak borrowing. In effect the historical results count the approximately 200 patients from I-SPY 1 as the equivalent of 40 I-SPY 2 patients.

Adjusting for time trends

In addition to the core logistic regression structure of the above terms, we include time trend parameters to capture the effect of possible drifting pCR rates over time.

Motivation: The initial statistical analyses in I-SPY 2 compared investigational arms with concurrently randomized controls (Park et al., 2016; Rugo et al., 2016). However, in September 2013, the FDA granted accelerated approval for pertuzumab + trastuzumab + docetaxel as neoadjuvant therapy for high risk HER2+ breast cancer. Our investigators and DSMB required dropping the I-SPY 2 control arm for HER2+ subtypes (trastuzumab + docetaxel) because it did not contain pertuzumab, which we did by amendment in early 2014. Going forward, we wanted to be able to use the results for the original control arm (trastuzumab plus docetaxel for HER2+, and docetaxel for HER2-) to assess the efficacy of new experimental arms but were concerned about the possibility of a drift in the pCR rates of the patient population over time and within patient subtype.

In response we modified the above Bayesian model with a time adjustment resulting in an overall "time machine" model that adjusts for any pCR drift that may occur over time within each arm and subtype. Having multiple arms in the trial with different time periods during which they are accruing patients enabled bridging across the different eras of trial accrual. The "time machine" discounts results from the past, with more discounting if they are further in the past. The mathematical basis and motivation for our approach to time adjustment is a statistical model for bridging eras in sports (Berry et al., 2012).

This model, described below, enables use of all available controls over all time periods in assessing efficacy of an experimental agent. We have used the time machine in all analyses in I-SPY 2 since Amendment #11 in July 2014, including for durvalumab + olaparib.

Time adjusted model (time machine)

We explicitly incorporate terms in the model to account for time trends in pCR response. This is done by using a set of time-dependent offset terms in the above Bayesian logistic model. Time is set to 0 at each analysis. We partition time in the past into bins of 90 days each. The index of the most recent bin, 0–90 days, is 1. The index of the bin 91–180 days in the past is 2. And so on.

Let t_i be the index of the bin for the randomization time of patient i. We model time-trend parameters $\delta(t)$ within each bin t. These are additive parameters in the model for the log-odds ratio of pCR rate. We use two sets of time-trend parameters, $\delta_+(t)$ for HER2-positive and $\delta_-(t)$ for HER2-negative. Consider patient i who has subtype (HR–, HER2+, MP–) and was randomized 750 days before present. Her bin t_i is 9 and her time-trend offset is $\delta_+(9)$.

We set $\delta_+(t) = \delta_-(t) = 0$ for $t = 1, 2, 3, 4$ which means that for a one-year period from the time of the analysis the pCR rate is assumed to be constant. Beyond a year in the past, we model the $\{\delta(t)\}$ as a second-order Normal Dynamic Linear Model (NDLM) (West and Harrison, 1997). This enables us to fit a 'smooth' effect over time. Suppressing the + and – subscripts, it has the following structure:

$$\delta(1) = \delta(2) = \ldots = \delta(4) = 0$$

$$\delta(5) \sim N(\mu_0, \tau_0^2)$$

$$\delta(6) - \delta(5) \sim N(\mu_1, \tau_1^2) \text{ for } t>6$$

$$\tau^2 \sim IG(\alpha, \beta)$$

For the priors in the model described above, the Normal priors are $N(\mu_0, \tau_0^2) = N(\mu_1, \tau_1^2)$= N(0,0.1) and $\alpha = 1$, $\beta = 0.001$for the Gamma priors.

After including the time trend component, the full Bayesian logistic regression model is:

$$y_i \sim Bernoulli(p_i)$$

$$logit(p_i) = \beta_0 + \beta_1 x_{1i} + \beta_2 x_{2i} + \beta_3 x_{3i} + \theta_{t_i} + \gamma_{1,t_i} x_{1i} + \gamma_{2,t_i} x_{2i} + \gamma_{3,t_i} x_{3i} + \delta_-(t_i) I(x_{2i} = 0) + \delta_+(t_i) I(x_{2i} = 1)$$

(Where $I()$ is the indicator function.)

Though in principle the time machine model can be applied at any time to the totality of results in I-SPY 2, the final efficacy analysis for any investigational arm includes only data available up until pathology results are complete for all patients in that arm (from all I-SPY 2 patients enrolled prior to arm closure). Although the model uses data from multiple investigational arms along with control, we only report the probability distribution of the specific investigational arm of interest and controls, and compute the probability that the pCR rate of that arm is greater than control and the predictive probabilities of success in a future trial (against control) for each biomarker signature. Comparisons between investigational arms are not reported or otherwise announced.

Biomarker analysis

Biomarker analysis in I-SPY2 employs a predefined 3-step Qualifying Biomarker Evaluation method (Wolf et al., 2017) First, we assess association of the biomarker with response in the experimental and control arms using a logistic model (likelihood ratio (LR) test $p < 0.05$). Relative performance between arms is assessed using a logistic model (biomarker × treatment interaction, likelihood ratio $p < 0.05$). If the biomarker × treatment interaction term coefficient is significant (LR $p < 0.05$), and if the predictive marker is significantly associated with response in the experimental arm (LR $p < 0.05$), the marker succeeds as a qualifying biomarker (QB). Analysis is also performed adjusting for HR status as a covariate, and numbers permitting, within receptor subsets. Our statistics are descriptive rather than inferential and do not adjust for multiplicities. pCR rates within MP1/2 classes are estimated using Bayesian logistic modeling. Analyses were performed in the computing environment R (v.3.6.3) using R Packages 'stats' (v.3.6.3), 'lmtest' (v.0.9–37), 'rjags' (v.4–10). Scripts are available upon request.

Cancer Cell, Volume *39*

Supplemental information

Durvalumab with olaparib and paclitaxel for high-risk HER2-negative stage II/III breast cancer: Results from the adaptively randomized I-SPY2 trial

Lajos Pusztai, Christina Yau, Denise M. Wolf, Hyo S. Han, Lili Du, Anne M. Wallace, Erica String-Reasor, Judy C. Boughey, A. Jo Chien, Anthony D. Elias, Heather Beckwith, Rita Nanda, Kathy S. Albain, Amy S. Clark, Kathleen Kemmer, Kevin Kalinsky, Claudine Isaacs, Alexandra Thomas, Rebecca Shatsky, Theresa L. Helsten, Andres Forero-Torres, Minetta C. Liu, Lamorna Brown-Swigart, Emmanuel F. Petricoin, Julia D. Wulfkuhle, Smita M. Asare, Amy Wilson, Ruby Singhrao, Laura Sit, Gillian L. Hirst, Scott Berry, Ashish Sanil, Adam L. Asare, Jeffrey B. Matthews, Jane Perlmutter, Michelle Melisko, Hope S. Rugo, Richard B. Schwab, W. Fraser Symmans, Doug Yee, Laura J. van't Veer, Nola M. Hylton, Angela M. DeMichele, Donald A. Berry, and Laura J. Esserman

SUPPLEMENTAL INFORMATION

Durvalumab with olaparib and paclitaxel for high-risk HER2 negative stage II/III breast cancer: Results from the adaptively randomized I-SPY2 platform trial

Pusztai et al.

SUPPLEMENTARY FIGURES

Figure S1: **CONSORT Diagram, describes study population, related to Table 1**

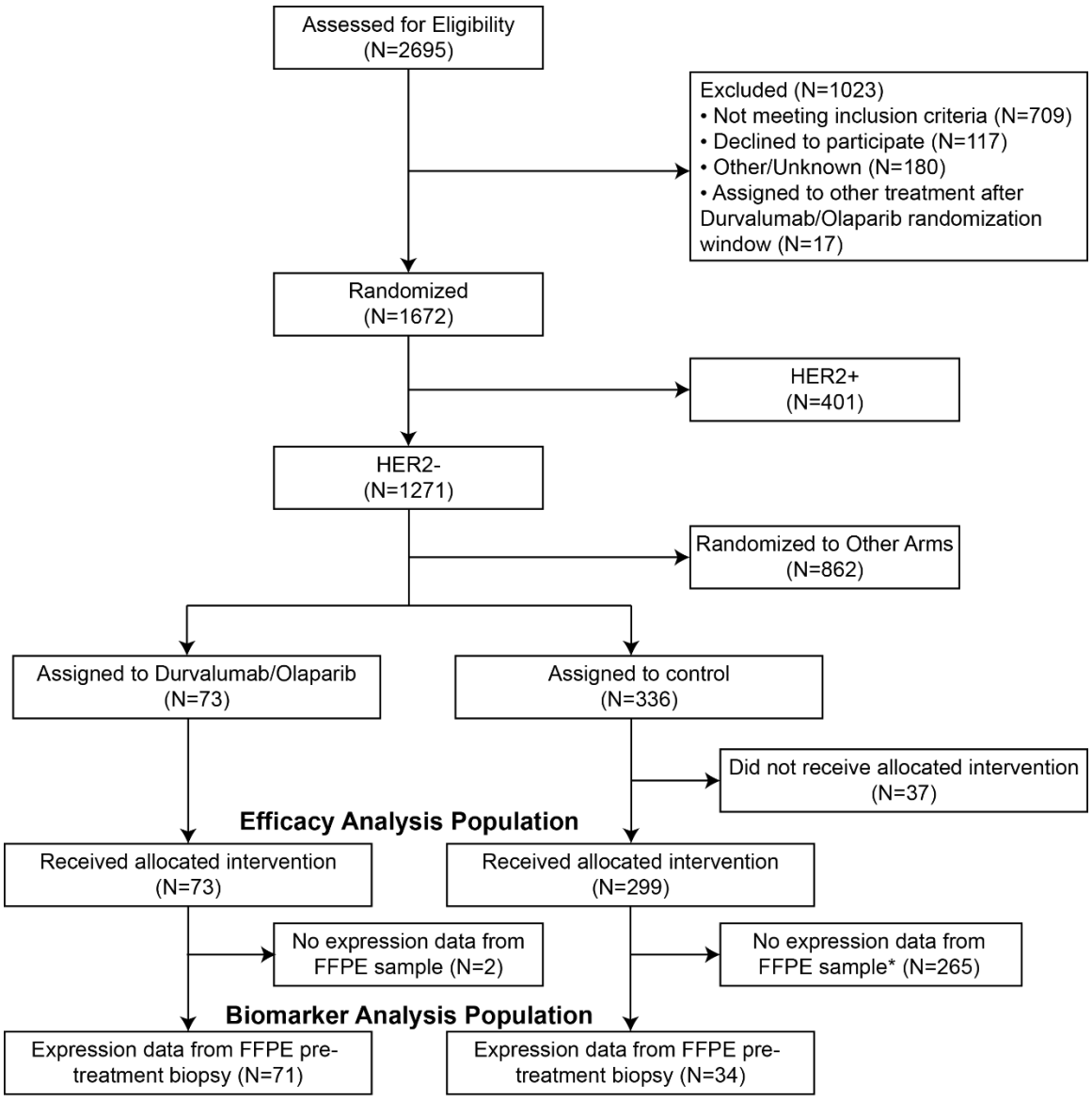

* I-SPY 2 began FFPE sample collection in May 2018. Control arm patients randomized prior to this date have expression data from fresh-frozen samples

Figure S2: Expression correlation matrix of gene signatures and genes, related to Figure 2. The heat map corresponds to Pearson correlation coefficients calculated across the entire biomarker study population included in this report (N=105, 71 in the experimental arm and 34 controls).

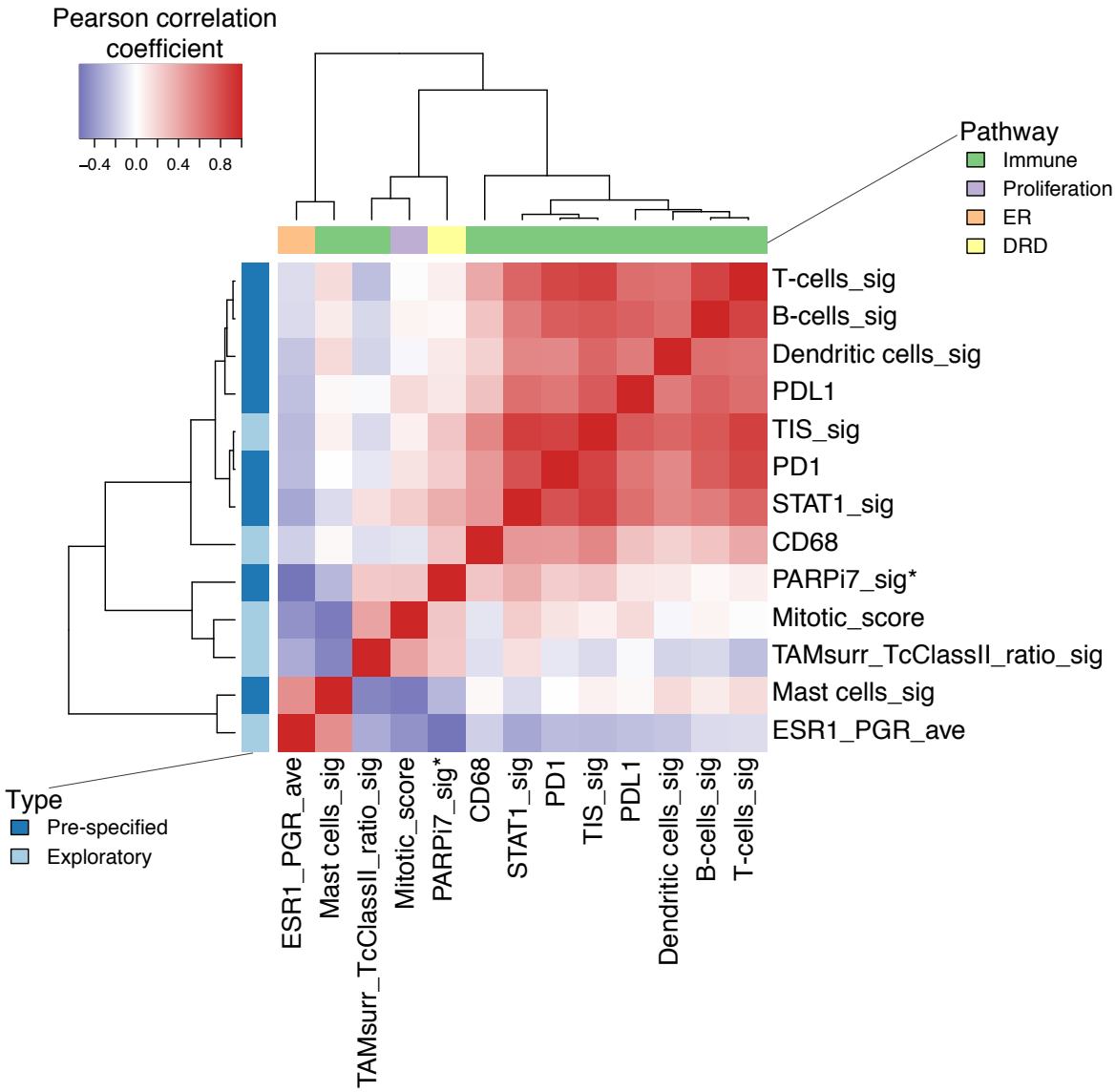

Figure S3**:** Expression of 13 mRNA biomarkers in cases with pathologic complete response (pCR) and no-PCR by treatment arm in the entire study population, related to Figure 2. Expression results are shown for all 105 cancers included in the biomarker study (N=71 experimental, N=34 controls)

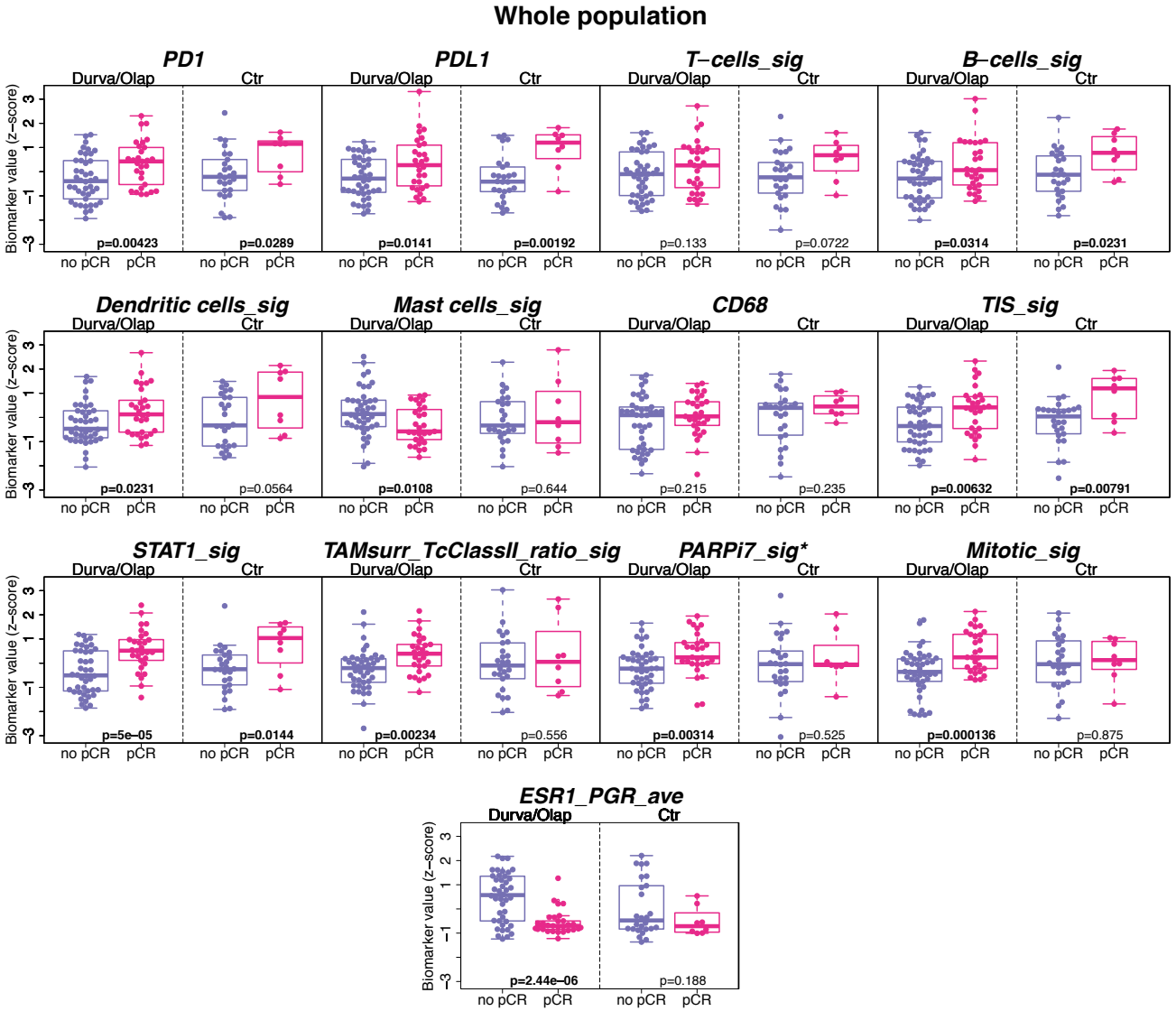

Figure S4**:** Expression of 13 mRNA biomarkers in cases with pathologic complete response (pCR) and no-PCR by treatment arm in TNBC, related to Figure 2. Expression results are shown for 40 TNBC cases (N=21 experimental, N= 19 controls).

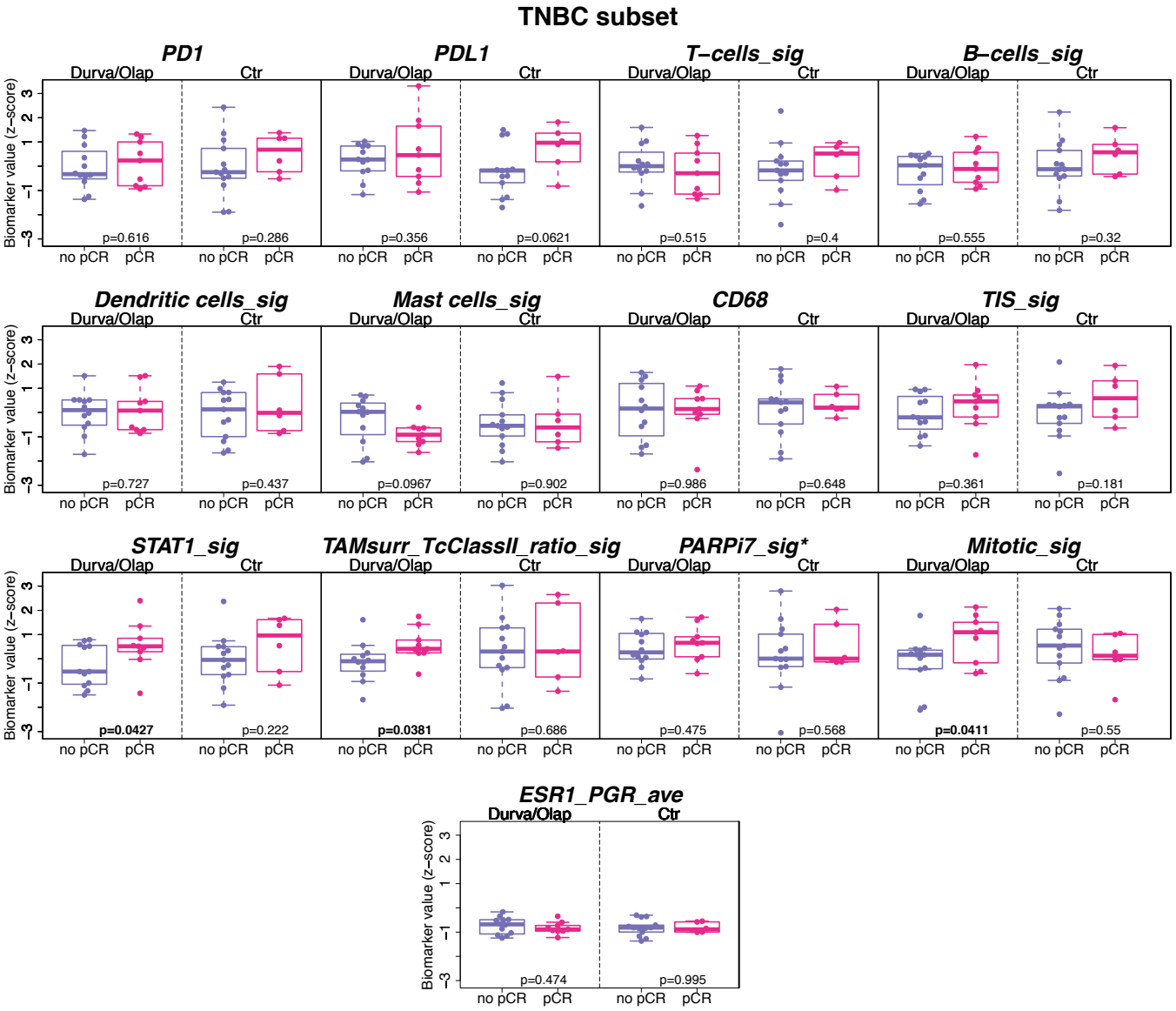

Figure S5**:** Expression of 13 mRNA biomarkers in cases with pathologic complete response (pCR) and no-PCR by treatment arm in the hormone receptor positive subset, related to Figure 2. Expression results are shown for the 65 HR+HER2- cancers subset (N=50 experimental arm, N=15 controls).

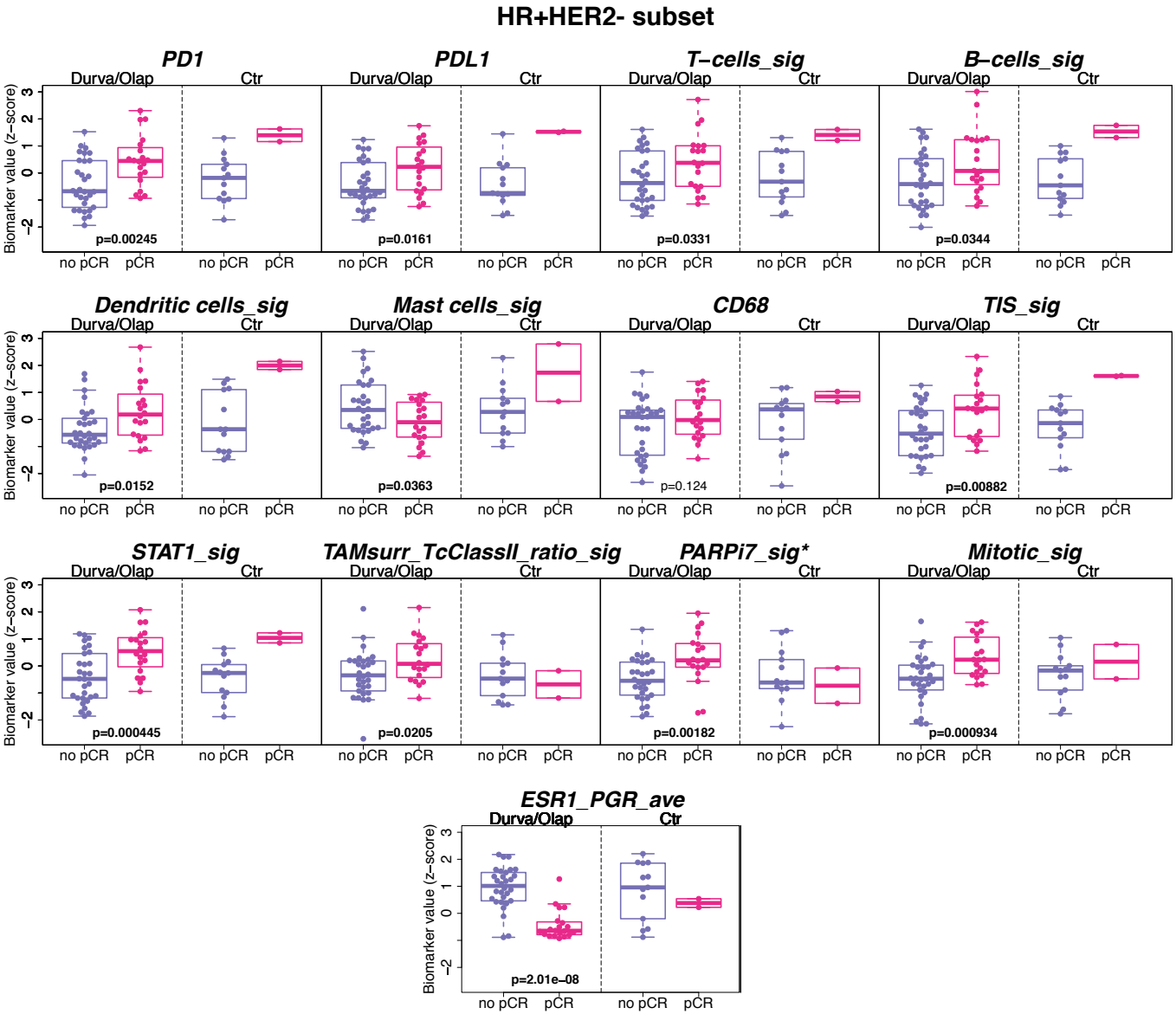

Figure S6: Residual cancer burden (RCB) categories and distribution of RCB scores by treatment arm in the MP1 and MP2 hormone receptor positive subtypes, related to Figure 3. Blue color bar indicates percent of cases with pCR, pink: RCB-I, magenta: RCB-II, red: RCB-II

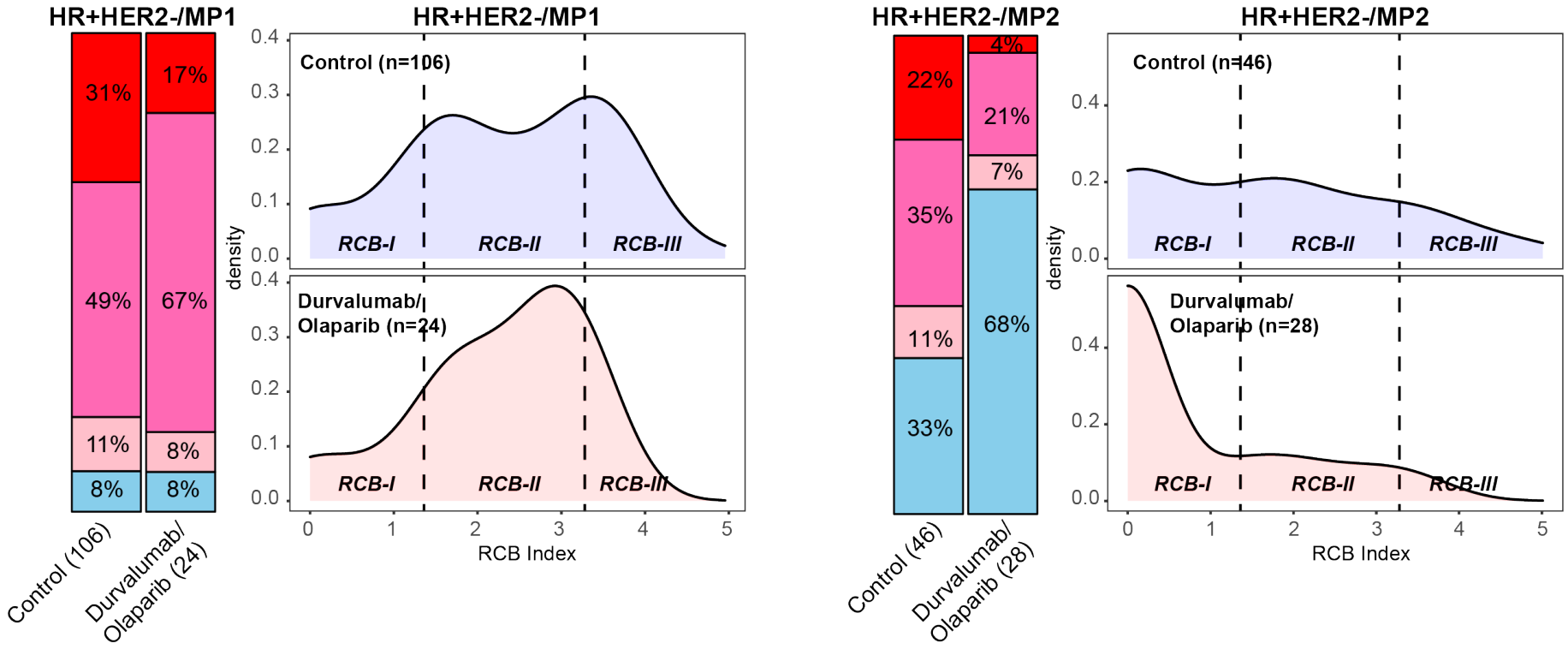

SUPPLEMENTARY TABLES

Table S1: Description and source of the 13 mRNA biomarkers, related to Figure 2 and 3.

Continuous mRNA biomarker	Type	Pathway	Genes	Scoring method	Publication
PD1	Pre-specified	Immune	PDCD1	Z-score (shift and scale so that mean=0, sd=1)	single gene
PDL1	Pre-specified	Immune	CD274	Z-score	single gene
T-cells signature	Pre-specified	Immune	CD3D, CD3E, CD3G, CD6, SH2D1A, TRAT1	1) Mean center data by gene, 2) average over genes, 3) Z-score	PMID:28239471
B-cells signature	Pre-specified	Immune	BLK, CD19, FCRL2, KIAA0125, MS4A1, PNOC, SPIB, TCL1A, TNFRSF17	1) Mean center, 2) average over genes, 3) Z-score	PMID:28239471
Dendritic cells signature	Pre-specified	Immune	CCL13, CD209, HSD11B1	1) Mean center, 2) average over genes, 3) Z-score	PMID:28239471
Mast cells signature	Pre-specified	Immune	CPA3, HDC, MS4A2, TPSAB1, TPSB2	1) Mean center, 2) average over genes, 3) Z-score	PMID:28239471
CD68	Exploratory	Immune	CD68	Z-score	single gene
TIS signature	Exploratory	Immune	TIGIT, CD27, CD8A, PDCD1LG2, CXCR6, LAG3, CD274, CMKLR1, NKG7, CCL5, PSMB10, ID01, PPBP, HLA-DQA1, CD276, STAT1, HLA-DRB1, HLA-E	1) Mean center, 2) average over genes, 3) Z-score	PMID: 28650338
STAT1 signature	Exploratory	Immune	TAP1, GBP1, IFIH1, PSMB9, CXCL9, IRF1, CXCL11, CXCL10, IDO1, STAT1	1) Mean center, 2) average over genes, 3) Z-score	PMID:19272155
TAMsurr_TcClassII ratio signature	Exploratory	Immune	TAMsurr: CXCL10, CXCL11, CCL8, LAMP3; TcClassII: CD2, CD3G, CD8A, IFNG, TNF, GZMB, GZMH, PRF1, ZAP70,	1) Mean center, 2) average over genes to calculate TAMsurr and TcClassII, then z-score each, 3) take log((TAMsurr+ adj)/(TcClassII+adj)), 4) Z-score. adj=abs(min(TAMsurr,TcClassII) + 1	PMID: 24205370

			HLA-DMA, HLA-DOA, HLA-DOB HLA-DPA1, HLA-DPB1 HLA-DQA1 HLA-DQB1 HLA-DQB2, HLA-DRA, HLA-DRB1, HLA-DRB2, HLA-DRB3, HLA-DRB4, HLA-DRB5, HLA-DRB6, CIITA, CD74		
revisedPARPi7 signature	Pre-specified	DNA repair	Prediction genes: Original (FF)= BRCA1, CHEK2, MAPKAPK2, MRE11A, NBN, TDG, XPA; Revised (FFPE)=BRCA1, CHEK2, MAPKAPK2, XRCC4, RAD17, POLB, CIRBP; Normalization genes: RPL24, ABI2, GGA1, E2F4, IPO8, CXXC1, RPS10	See implementation of FFPE revised PARPi7 in STAR Methods	PMID: 22875744; PMID:28948212
Mitotic signature	Exploratory	Proliferation	PLK1, CDK1, BUB1B, NEK2, TTK, MELK, PLK4, CHEK1, AURKA, AURKB, BUB1, PBK	1) Mean center, 2) average over genes, 3) Z-score	PMID: 24060333
ESR1_PGR average	Exploratory	ER	ESR1, PGR	1) Mean center, 2) average over genes, 3) Z-score	average of 2 genes

Table S2: Association between 13 mRNA biomarkers and pathologic response in the whole biomarker study population and in the TNBC and HR+/HER- subsets, related to Figure 2. Exp and QB indicate exploratory and qualifying biomarkers, respectively. OR, HR and LR p stand for odds ratio, hazard ratio, and logistic regression p value, respectively.

Immune signature	Type	Pathway	Whole population (n=105)						TN subset (n=40)				HR+HER2- subset	
			Durvalumab/Olaparib arm (n=71)			Control arm (n=34)		treatment interaction	Durvalumab/Olaparib arm (n=21)		Control arm (n=19)		Durvalumab/Olaparib arm (n=50)	
			OR/unit	LR p	LR p (adj HR)	OR/unit	LR p	LR p	OR/unit	LR p	OR/unit	LR p	OR/unit	LR p
ESR1_PGR_ave	Exp	ER	0.22 [0.09-0.45]	**2.44E-06**	**2.26E-08**	0.55 [0.16-1.3]	0.188	0.188	0.34 [0.014-6.31]	0.474	0.99 [0.029-32.5]	0.995	0.082 [0.019-0.24]	**2.01E-08**
STAT1_sig	QB	Immune	3.15 [1.75-6.37]	**5.00E-05**	**5.12E-05**	3.02 [1.23-9.78]	**0.0144**	0.944	2.86 [1.03-11.9]	**0.0427**	1.8 [0.71-5.57]	0.222	3.27 [1.63-7.7]	**0.000445**
Mitotic_sig	Exp	Proliferation	3.03 [1.65-6.34]	**0.000136**	**0.000109**	1.06 [0.49-2.42]	0.875	**0.0455**	2.67 [1.04-10]	**0.0411**	0.77 [0.30-1.87]	0.55	3.56 [1.6-9.93]	**0.000934**
TAMsurr_TcClassII_ratio_sig	Exp	Immune	2.58 [1.37-5.41]	**0.00234**	**0.00234**	1.21 [0.63-2.33]	0.556	0.104	3.91 [1.07-26.8]	**0.0381**	1.15 [0.57-2.44]	0.686	2.3 [1.13-5.38]	**0.0205**
PARPi7*_sig	QB	DRD	2.37 [1.32-4.65]	**0.00314**	**0.00212**	1.25 [0.63-2.63]	0.525	0.183	1.58 [0.45-6.24]	0.475	1.27 [0.57-3.24]	0.568	3.16 [1.49-8.13]	**0.00182**
PD1	QB	Immune	2.12 [1.26-3.81]	**0.00423**	**0.00431**	2.59 [1.1-7.62]	**0.0289**	0.717	1.29 [0.47-3.68]	0.616	1.66 [0.66-4.99]	0.286	2.6 [1.38-5.61]	**0.00245**
TIS_sig	Exp	Immune	2.06 [1.22-3.74]	**0.00632**	**0.0065**	3.62 [1.35-13.3]	**0.00791**	0.357	1.61 [0.59-5.17]	0.361	2.03 [0.74-7.57]	0.181	2.26 [1.22-4.67]	**0.00882**
Mast cells_sig	QB	Immune	0.49 [0.26-0.86]	**0.0108**	**0.00796**	1.18 [0.56-2.47]	0.644	0.0629	0.38 [0.098-1.18]	0.0967	1.07 [0.35-3.12]	0.902	0.48 [0.22-0.96]	**0.0363**
PDL1	QB	Immune	1.9 [1.13-3.38]	**0.0141**	**0.0131**	4.12 [1.61-14.2]	**0.00192**	0.176	1.5 [0.64-4.13]	0.356	2.66 [0.96-9.9]	0.0621	2.25 [1.16-4.77]	**0.0161**
Dendritic cells_sig	QB	Immune	1.86 [1.09-3.37]	**0.0231**	**0.0237**	2.07 [0.98-5.07]	0.0564	0.83	1.2 [0.42-3.62]	0.727	1.47 [0.56-4.33]	0.437	2.2 [1.16-4.67]	**0.0152**
B-cells_<avg>_sig	QB	Immune	1.7 [1.05-2.92]	**0.0314**	**0.0296**	2.87 [1.14-9.43]	**0.0231**	0.352	1.44 [0.43-5.47]	0.555	1.71 [0.60-6.05]	0.32	1.78 [1.04-3.28]	**0.0344**
T-cells_<avg>_sig	QB	Immune	1.45 [0.90-2.41]	0.133	0.13	2.19 [0.94-6.33]	0.0722	0.427	0.72 [0.25-1.92]	0.515	1.54 [0.57-5.14]	0.4	1.87 [1.05-3.56]	**0.0331**
CD68	Exp	Immune	1.36 [0.84-2.28]	0.215	0.221	1.74 [0.72-5.44]	0.235	0.658	0.99 [0.43-2.33]	0.986	1.28 [0.45-4.38]	0.648	1.62 [0.88-3.21]	0.124